AD-A104 685 ARMY ELECTRONICS RESEARCH AND DEVELOPMENT COMMAND FO--ETC F/G 20/3
EVALUATION OF ALPHA ALUMINUM PHOSPHATE FOR ADVANCED ACOUSTIC WA--ETC(U)
AUG 81 J GUALTIERI, A BALLATO
UNCLASSIFIED DELET-TR-81-15 NL

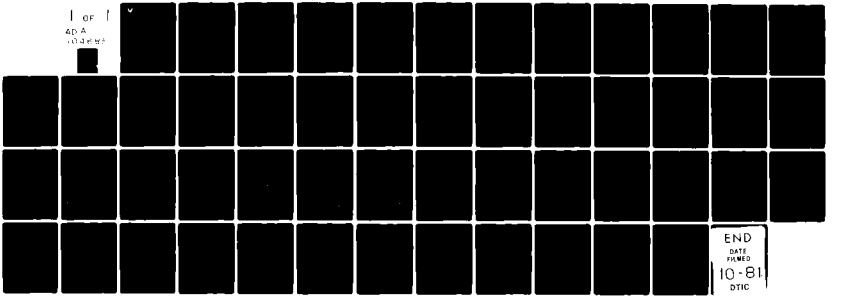

END
DATE FILMED
10-81
DTIC

AD A104685

LEVEL

(12)

RESEARCH AND DEVELOPMENT TECHNICAL REPORT

DELET-TR-81-15

EVALUATION OF ALPHA ALUMINUM PHOSPHATE FOR ADVANCED ACOUSTIC WAVE DEVICES

DTIC ELECTE SEP 29 1981 H

JOHN GUALTIERI
ARTHUR BALLATO
ELECTRONICS TECHNOLOGY & DEVICES LABORATORY

AUGUST 1981

DISTRIBUTION STATEMENT
Approved for public release;
distribution unlimited.

DTIC FILE COPY

ERADCOM
US ARMY ELECTRONICS RESEARCH & DEVELOPMENT COMMAND
FORT MONMOUTH, NEW JERSEY 07703

58

NOTICES

Disclaimers

The citation of trade names and names of manufacturers in this report is not to be construed as official Government indorsement or approval of commercial products or services referenced herein.

Disposition

Destroy this report when it is no longer needed. Do not return it to the originator.

UNCLASSIFIED

SECURITY CLASSIFICATION OF THIS PAGE (When Data Entered)

REPORT DOCUMENTATION PAGE	READ INSTRUCTIONS BEFORE COMPLETING FORM
1. REPORT NUMBER: DELET-TR-81-15	2. GOVT ACCESSION NO.: AD-A104685
	3. RECIPIENT'S CATALOG NUMBER
4. TITLE (and Subtitle): EVALUATION OF ALPHA ALUMINUM PHOSPHATE FOR ADVANCED ACOUSTIC WAVE DEVICES.	5. TYPE OF REPORT & PERIOD COVERED: Technical Report
	6. PERFORMING ORG. REPORT NUMBER
7. AUTHOR(s): JOHN GUALTIERI, ARTHUR BALLATO	8. CONTRACT OR GRANT NUMBER(s)
9. PERFORMING ORGANIZATION NAME AND ADDRESS: US Army Elct Tech & Devices Laboratory (ERADCOM) ATTN: DELET-MA Fort Monmouth, NJ 07703	10. PROGRAM ELEMENT, PROJECT, TASK AREA & WORK UNIT NUMBERS: 1L1 62705 AH94 09
11. CONTROLLING OFFICE NAME AND ADDRESS: US Army Elct Tech & Devices Laboratory (ERADCOM) ATTN: DELET-MA Fort Monmouth, NJ 07703	12. REPORT DATE: August 1981
	13. NUMBER OF PAGES: 46
14. MONITORING AGENCY NAME & ADDRESS(if different from Controlling Office)	15. SECURITY CLASS. (of this report): Unclassified
	15a. DECLASSIFICATION/DOWNGRADING SCHEDULE

16. DISTRIBUTION STATEMENT (of this Report)

Approved for public release; distribution unlimited.

17. DISTRIBUTION STATEMENT (of the abstract entered in Block 20, if different from Report)

18. SUPPLEMENTARY NOTES

19. KEY WORDS (Continue on reverse side if necessary and identify by block number)

Crystal resonators	Alpha aluminum phosphate
Crystal oscillators	Berlinite
Piezoelectric crystals	Frequency control
Piezoelectric vibrators	Acoustic wave devices

20. ABSTRACT (Continue on reverse side if necessary and identify by block number)

Alpha aluminum phosphate (berlinite) has been investigated as a highly piezoelectric material potentially suitable for use in advanced bulk and surface acoustic wave devices. Areas of investigation include: (1) crystal structure, (2) methods of crystal growth, (3) defects in structure, (4) the presence of water impurities, (5) piezoelectric resonators, and (6) the equivalent electrical circuit. Calculations have been carried out for frequency constant, piezoelectric coupling factor, and linear temperature coefficient as functions of orientation for general, doubly rotated plate orientations, and disclose

DD FORM 1 JAN 73 1473 EDITION OF 1 NOV 65 IS OBSOLETE

Unclassified

SECURITY CLASSIFICATION OF THIS PAGE (When Data Entered)

Item #20 ABSTRACT (CONTINUED)

quartz-like properties with coupling factors appreciably larger than quartz. Measurements indicate larger than expected losses, indicative of incorporation of impurities during growth; suggestions for further work are given.

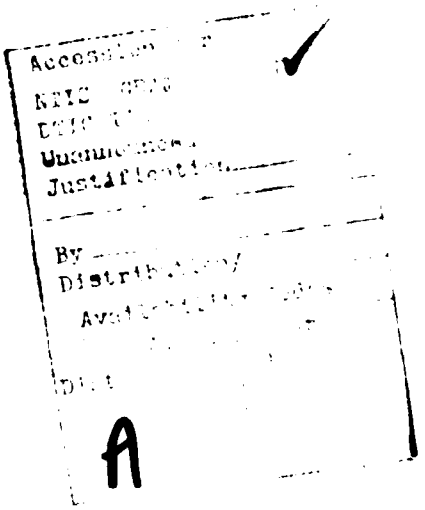

CONTENTS

PAGE

INTRODUCTION 1

CRYSTAL STRUCTURE. 6

CRYSTAL GROWTH 12

DEFECTS. 12

THE H_2O IMPURITY 14

RESONATORS 15

THE EQUIVALENT CIRCUIT 29

REFERENCES 45

FIGURES:

1. Singly and doubly rotated plates 2
2. Frequency constants of (YXℓ)θ quartz and berlinite . . . 3
3. Coupling factors of (YXℓ)θ quartz and berlinite. 4
4. Typical surface wave device. 7
5. Surface wave motion and electric field coupling. 8
6. Coupling factors squared of (YXℓ)θ quartz and berlinite. 9
7. Structure of dextro-rotary quartz and berlinite. 10
8. Structure of laevo-rotary quartz and berlinite 11
9. Electrical and optical twinning. 13
10. IR transmittance of quartz and berlinite 16
11. Frequency constants of (YXwℓ) $0^o/\theta$ berlinite 17
12. Frequency constants of (YXwℓ) $6^o/\theta$ berlinite 18
13. Frequency constants of (YXwℓ) $12^o/\theta$ berlinite. 19
14. Frequency constants of (YXwℓ) $18^o/\theta$ berlinite. 20
15. Frequency constants of (YXwℓ) $24^o/\theta$ berlinite. 21
16. Frequency constants of (YXwℓ) $30^o/\theta$ berlinite. 22

17. Coupling factors of (YXwℓ) 0°/θ berlinite. 23

18. Coupling factors of (YXwℓ) 6°/θ berlinite. 24

19. Coupling factors of (YXwℓ) 12°/θ berlinite 25

20. Coupling factors of (YXwℓ) 18°/θ berlinite 26

21. Coupling factors of (YXwℓ) 24°/θ berlinite 27

22. Coupling factors of (YXwℓ) 30°/θ berlinite 28

23. Temperature coefficients of (YXwℓ) 0°/θ berlinite. . . . 30

24. Temperature coefficients of (YXwℓ) 6°/θ berlinite. . . . 31

25. Temperature coefficients of (YXwℓ) 12°/θ berlinite . . . 32

26. Temperature coefficients of (YXwℓ) 18°/θ berlinite . . . 33

27. Temperature coefficients of (YXwℓ) 24°/θ berlinite . . . 34

28. Temperature coefficients of (YXwℓ) 30°/θ berlinite . . . 35

29. Loci of zero temperature coefficient for berlinite . . . 36

30. Frequency constants for (YXw)ϕ berlinite 37

31. Coupling factors for (YXw)ϕ berlinite. 38

32. Mode spectrograph of berlinite resonance 39

33. Block diagram of measurement 40

34. Equivalent electrical network. 41

TABLES:

1. Frequency constants N and piezoelectric coupling factors k for (YXℓ)θ cuts of quartz and berlinite. 5

2. Rotated Y-cut, pure shear mode, crystal class 32 14

3. Frequency constants and coupling factors of the thickness modes of X- and Y-cut berlinite 29

INTRODUCTION

Alpha-aluminum phosphate, also known as the mineral berlinite, occurs in rare deposits as a massive, granular material. In natural formations, the individual crystallites are sub-millimeter in size. Alpha-aluminum phosphate (α - $A\ell\ PO_4$) is isotypic with quartz (α - $Si\ O_2$). The two materials show a number of similarities with regard to their properties. For example, the growth habits of synthesized crystals are similar in that both display minor $\{10\bar{1}1\}$ and major $\{01\bar{1}1\}$ rhombohedra. Quartz also shows prism $\{10\bar{1}0\}$ faces that rarely occur in α - $A\ell\ PO_4$. The cleavage tendencies (on a microscopic scale) are related, quartz showing $\{10\bar{1}0\}$ and rhombohedral $\{10\bar{1}1\}$ cleavage, while α - $A\ell\ PO_4$ displays only rhombohedral cleavage and partial microcleavage along the $[1\bar{2}10]$ zone in the neighborhood of $\{10\bar{1}1\}$[1]*. The hardnesses are different, and this is manifest in the grinding and polishing times required to finish crystal plates. Alpha-$A\ell\ PO_4$ plates are finished in 10 to 20% of the time necessary to finish quartz. Also, Knoop indentation hardnesses of quartz and α - $A\ell\ PO_4$ are ~1000 and ~450, respectively. The mass densities of both materials are nearly equal, and their optical properties are similar. The acoustic velocity range of α- $A\ell\ PO_4$ is about 15% lower than quartz, and the ratios of corresponding elastic constants are very uniform. The dielectric permittivities of quartz are about 30% lower than those of berlinite. Where the two materials differ substantially is in their piezoelectric constants, where berlinite enjoys a two- or three-fold advantage. This translates into a similar advantage in the piezoelectric coupling factor which governs the electromechanical transduction efficiency.

The coupling factor advantage of α - $A\ell\ PO_4$ over quartz would have little practical value unless temperature-compensated crystal cuts existed as they do for quartz. Here again, the isotypism of berlinite and quartz appears to be a sufficient condition. For example, temperature compensation in this crystal structure (class 32) depends upon the anomalous (positive) value of $\partial c_{66}/\partial T$, which is related to the rotation of MO_4 (M = metal) tetrahedra under thermal expansion; (c_{66} relates a shear stress about the z axis to a shear strain about the same axis). Materials with open structures in which sizeable rotations can occur are candidates for positive temperature coefficients, and therefore probable temperature compensation[2]*. Rotated-Y-cut plates have the configuration shown in (a) of Figure 1; a comparison of the frequency constant (one-half the acoustic velocity) and piezoelectric (electromechanical) coupling coefficient for the active mode of such plates in quartz and berlinite is given, respectively, in Figure 2 and Figure 3, and tabulated in Table 1.

Other materials surpass α - $A\ell\ PO_4$ in coupling factor; for example, lithium niobate, but the attractive combination of strong coupling and temperature compensation of the acoustic velocity is absent in $Li\ Nb\ O_3$. Piezoelectric coupling factors substantially

---

* See list of references beginning on page 45.

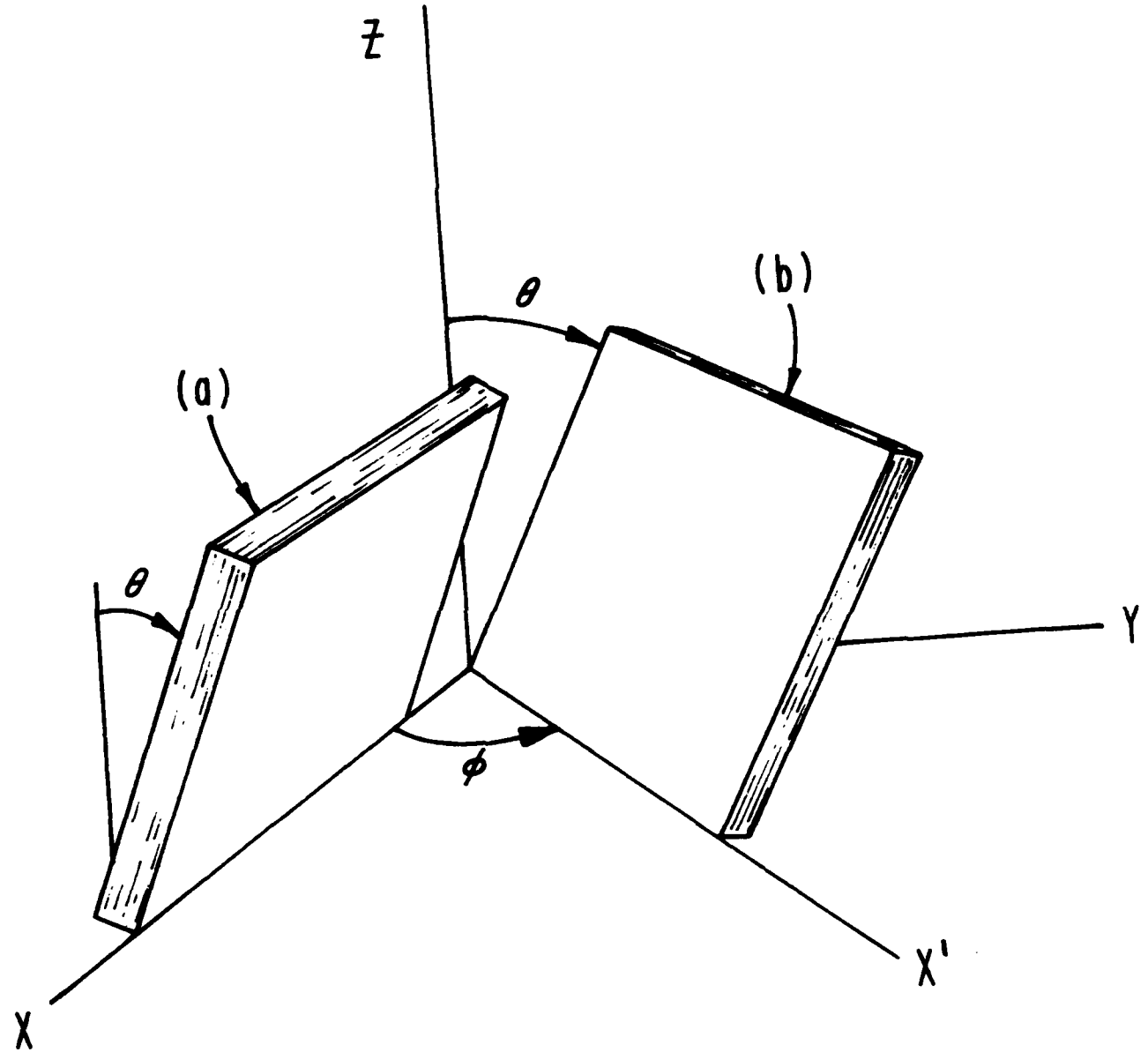

FIGURE 1. SINGLY AND DOUBLY ROTATED PLATES

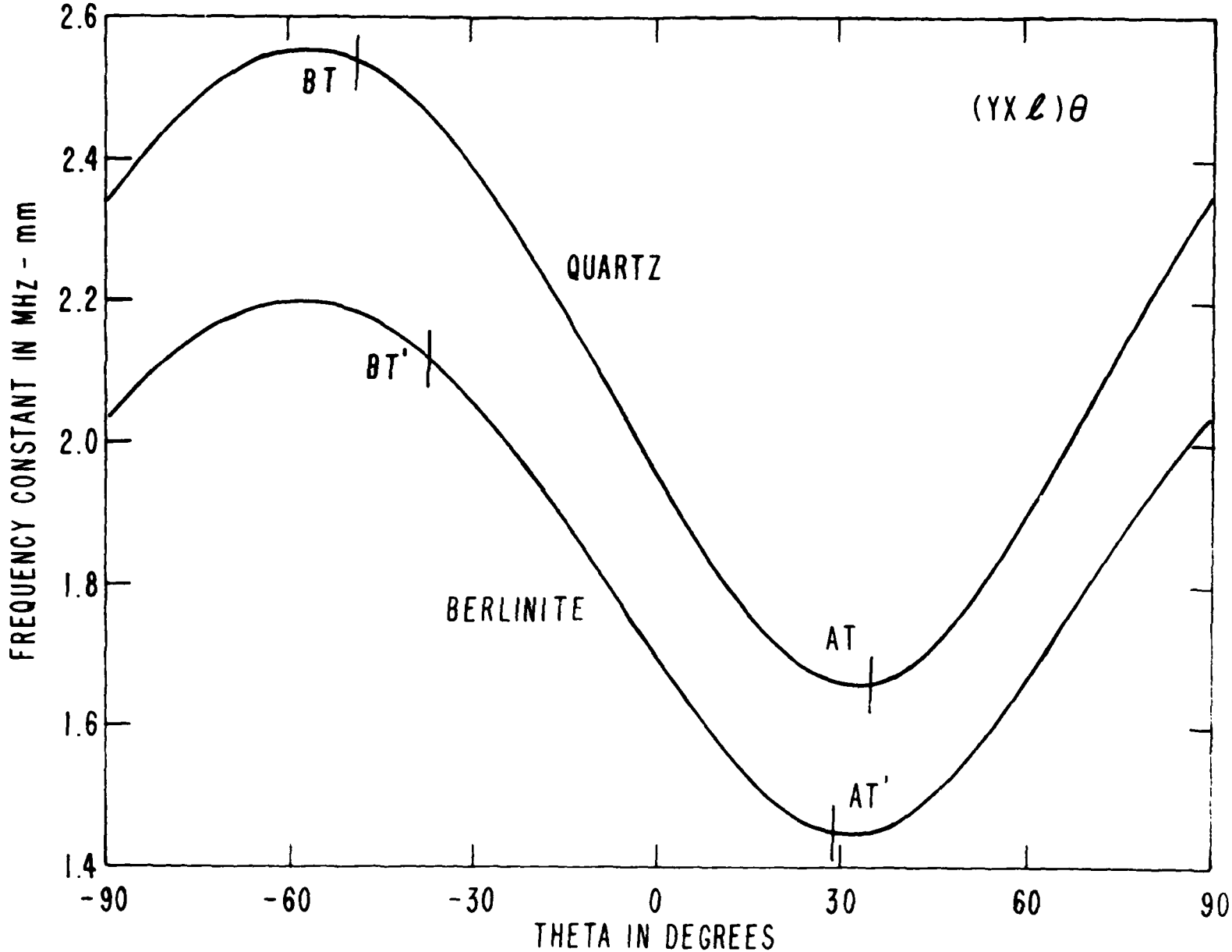

FIGURE 2. FREQUENCY CONSTANTS OF (YXℓ)θ QUARTZ AND BERLINITE

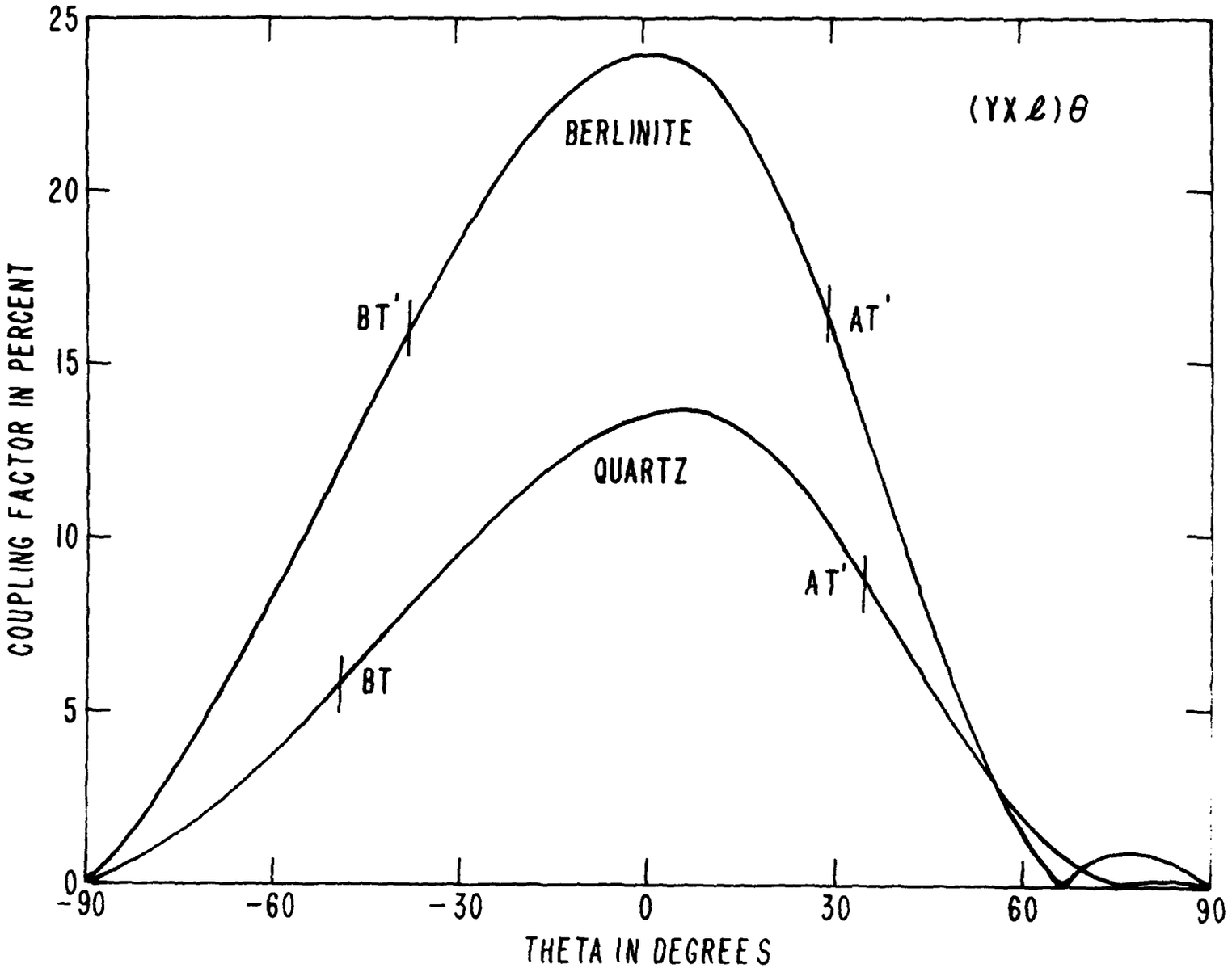

FIGURE 3. COUPLING FACTORS OF (YXℓ)θ QUARTZ AND BERLINITE

TABLE 1

FREQUENCY CONSTANTS N AND PIEZOELECTRIC COUPLING FACTORS k FOR (YXℓ)θ CUTS OF QUARTZ AND BERLINITE.

CUT		θ	N	|k|	k^2
		DEGREES	MHz-mm	PERCENT	PERCENT
BERLINITE	AT'	28.6	1.448	16.5	2.73
	BT'	-37.3	2.118	16.1	2.60
	Y	0	1.696	24.0	5.74
	Z	± 90	2.030	0	0
QUARTZ	AT	35.25	1.661	8.80	0.77
	BT	-49.20	2.536	5.62	0.32
	Y	0	1.958	13.5	1.84
	Z	± 90	2.338	0	0

larger than quartz, along with good temperature stability, permit the fabrication of both bulk and surface acoustic wave (SAW) devices with enhanced capabilities. A typical SAW delay line device is depicted in Figure 4; an alternating voltage applied between the interdigitated fingers of one port produces the wave motion shown in Figure 5. The second port produces, by the same piezoelectric effect, the voltage waveform delayed by the propagation time between the input and output structures. The structures become resonant at frequencies such that the acoustic wavelength is commensurate with the finger spacings. By controlling the finger lengths, widths, spacings, and polarities, sophisticated signal processing functions may be performed in a microcircuit-compatible, planar configuration. Among the bulk or SAW devices of interest are voltage-controlled crystal oscillators (VCXOs) with increased tuning (pulling) range, temperature-compensated crystal oscillators (TCXOs) that operate well on harmonics because of increased coupling, convolvers, correlators, coupled-mode bulk and SAW filters, resonators and delay lines, encoders and decoders, and other signal processing devices. For such devices, the parameter of importance is not simply the coupling, but rather its square; the comparison of Figure 3 is given in terms of coupling squared in Figure 6. Because of the high applications potential of berlinite in this regard, it has become the object of considerable interest. References 1-22* can be applied to the problems associated with berlinite and alpha quartz.

CRYSTAL STRUCTURE

The crystal structure of α - $A\ell PO_4$ is isotypic with that of α - quartz; in the latter structure, the Si atoms are layered in planes perpendicular to the c-axis. In the α - $A\ell PO_4$ structure, atoms of $A\ell$ and P comprise alternate layers. Thus, half of the Si positions are "replaced" by $A\ell$ and the other half by P. This results in a doubling of the unit cell along the c axis. In either structure the MO_4 tetrahedra are arranged in the form of a screw around the three-fold c axis. Both a left-screw and a right-screw are possible; these enantiomorphic forms are shown, respectively, in Figure 7 and Figure 8. This structure has been described, sometimes incorrectly, using various axial systems called settings[3]. The setting endorsed by most communications engineers and workers in the field of quartz crystal structure is the Z (+) setting. In this setting the minor rhombohedra, Z, are indexed $(10\bar{1}1)$ and the two-fold axis along which the Z axis is chosen develops a positive charge at its positive end on extension. This setting uses a right-handed coordinate system (RHCS) for right-quartz (dextrorotary) and a left-handed coordinate system (LHCS) for left-quartz (laevorotary). It should be understood that dextrorotary (optical) refers to a left-screw (LS) (physical), and laevorotary (optical) refers to a right-screw (RS) (physical). Donnay and LePage[3] proposed a coordinate system whose handedness matches that of the crystallographic (physical) screw. This convention, we feel, would be very difficult to establish in the field of communications

---

* See list of references beginning on page 45.

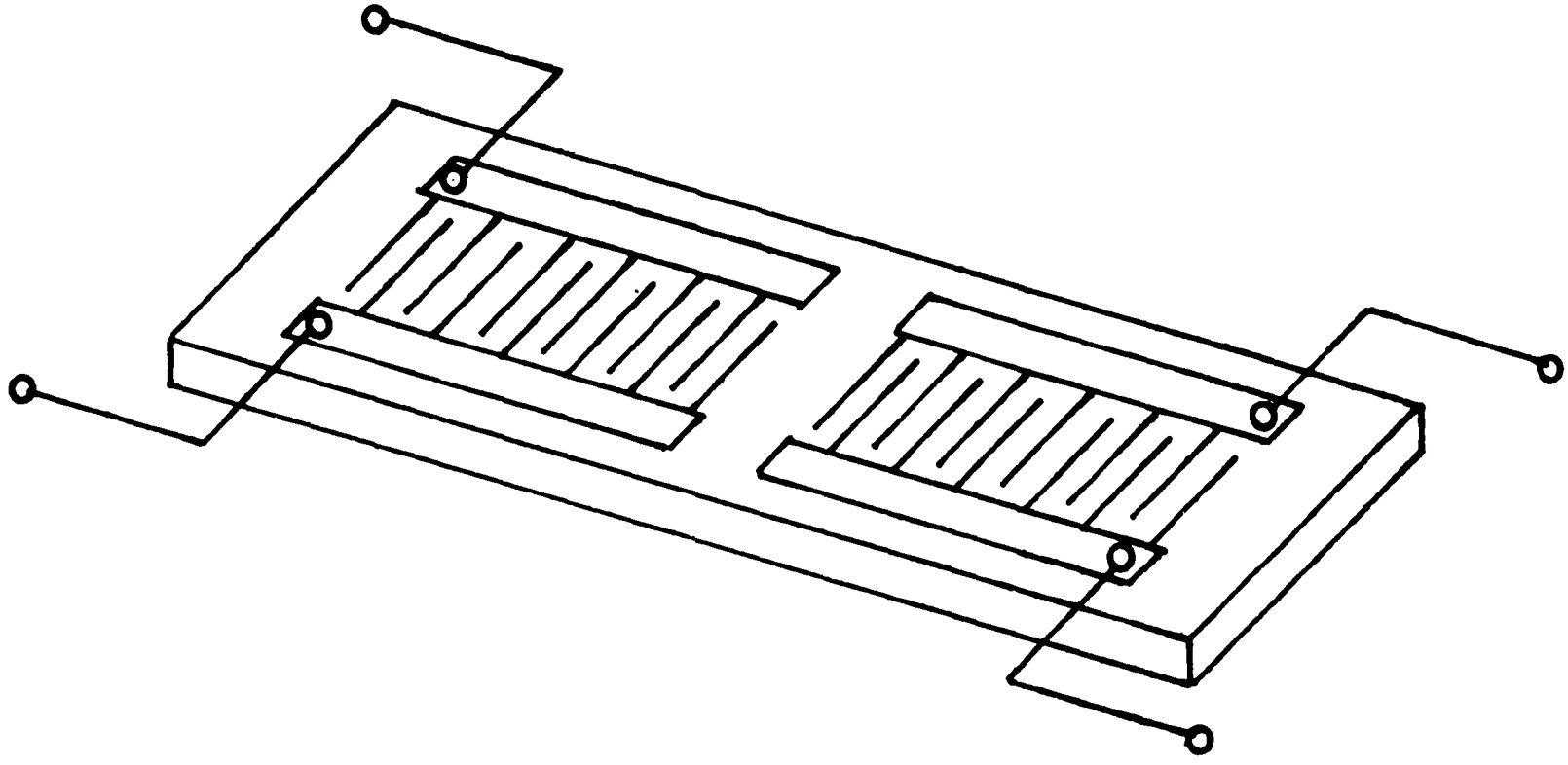

FIGURE 4. TYPICAL SURFACE WAVE DEVICE

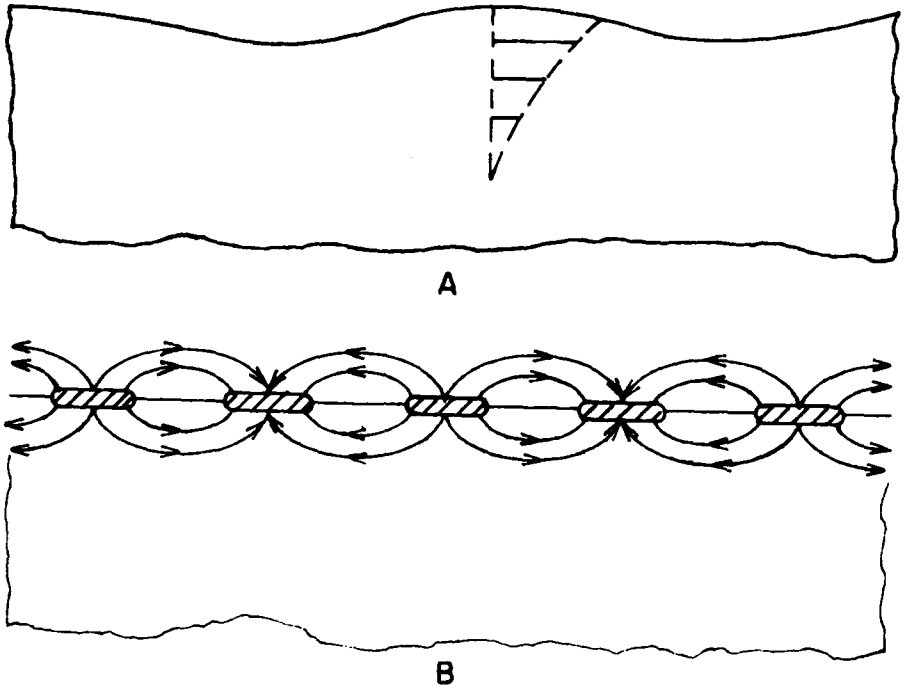

A. WAVE MOTION
B. ELECTRIC FIELD COUPLING

FIGURE 5. SURFACE WAVE MOTION AND ELECTRIC FIELD COUPLING

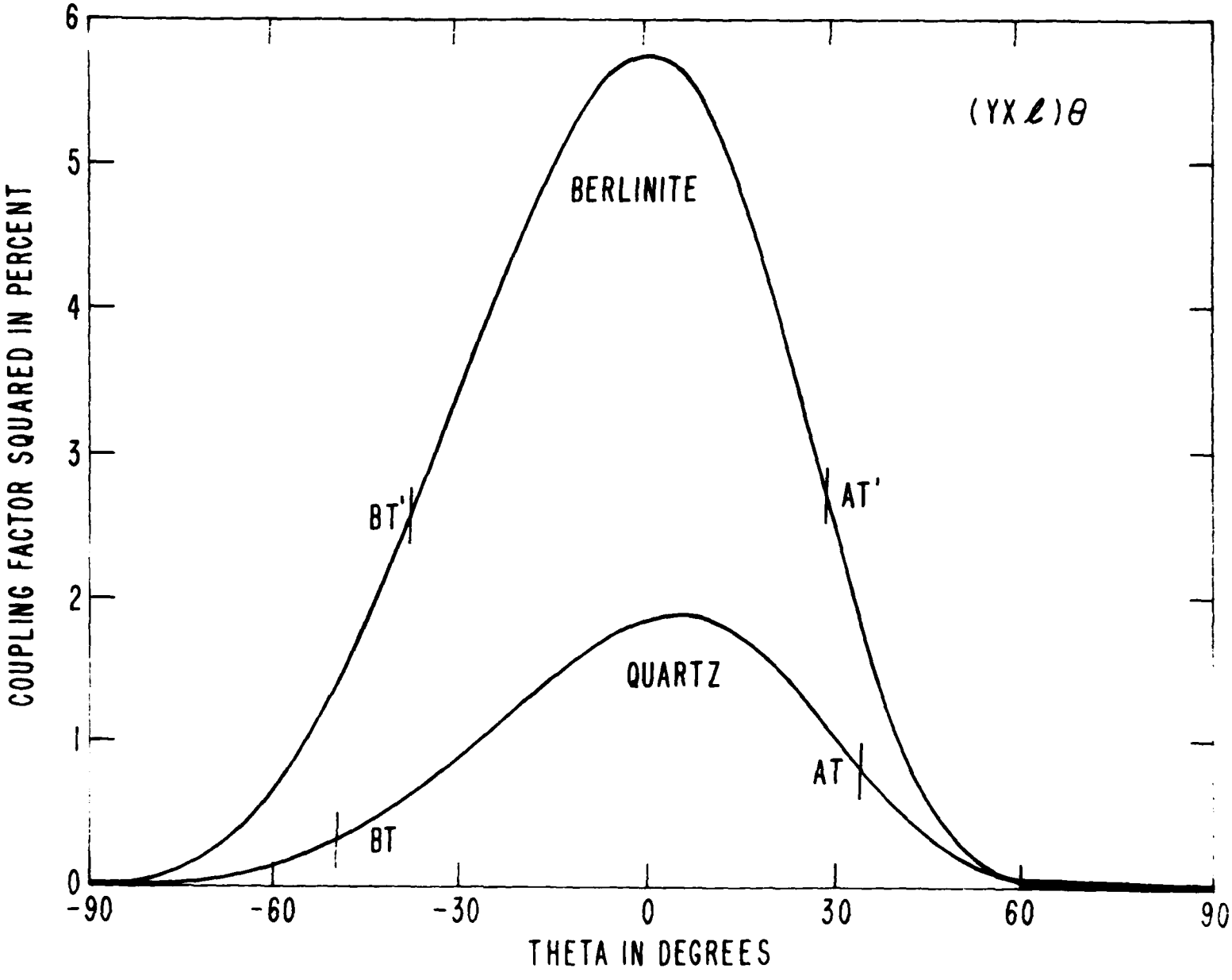

FIGURE 6. COUPLING FACTORS SQUARED OF (YXℓ)° QUARTZ AND BERLINITE

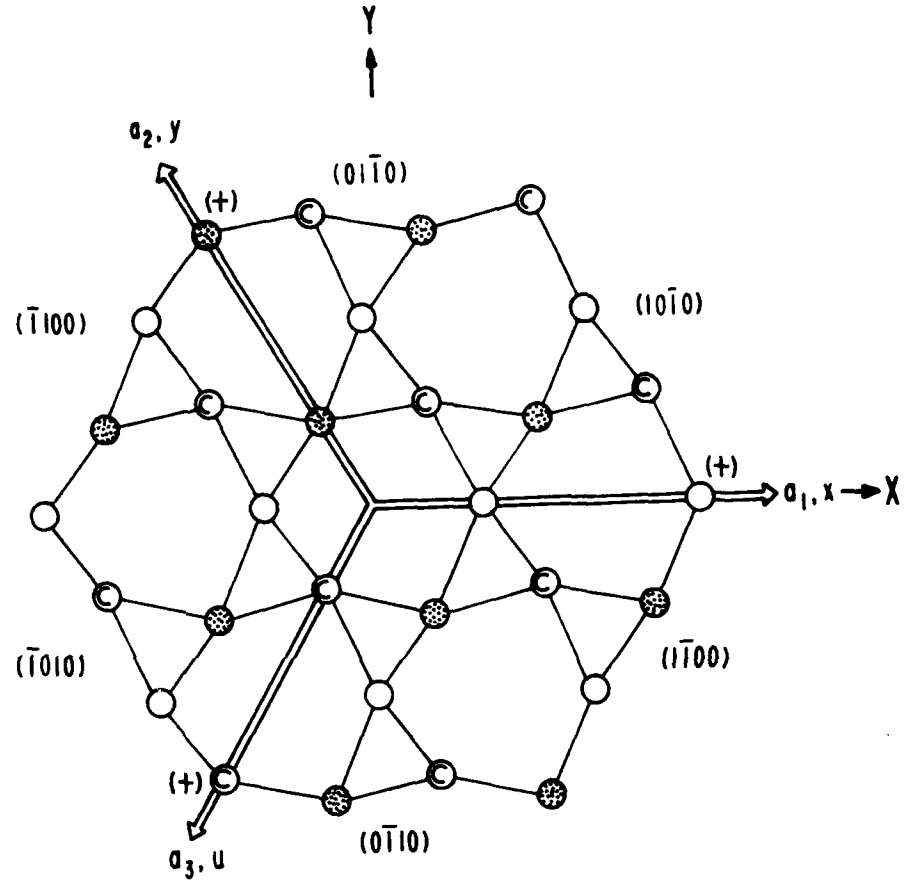

FIGURE 7. STRUCTURE OF DEXTRO-ROTARY QUARTZ AND BERLINITE

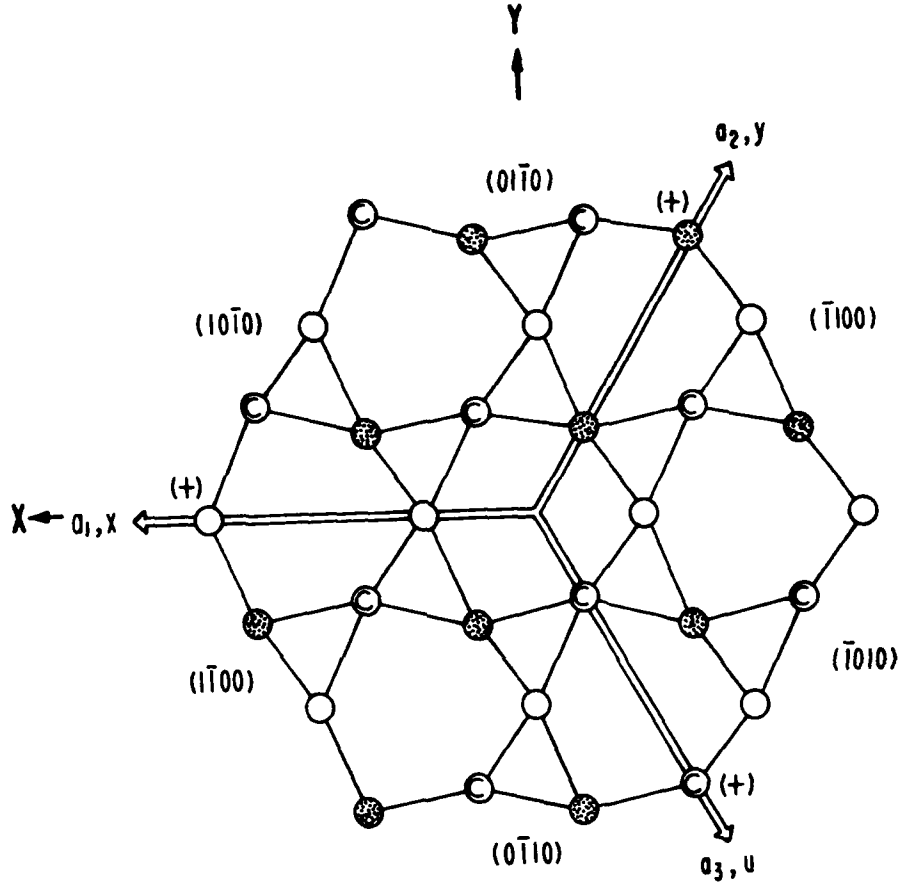

○ Si Al at 0 LH(laevo-rotary) X,Y,Z piezoelectric axes

◎ Si P at 1/3c RS +Z,+Z,c perpendicular to plane of diagram

◉ Si Al at 2/3c LHCS

z indexed (10$\bar{1}$1)

(+) on extension

FIGURE 8. STRUCTURE OF LAEVO-ROTARY QUARTZ AND BERLINITE

engineering given the international familiarity with the Z (+) setting.

Unfortunately, the latest IEEE Standard on Piezoelectricity[15] establishes a Z (-) setting for left-quartz (RHCS for RS) and a Z (+) setting for right-quartz (RHCS for LS). The atomic positions, sites, and fractional coordinates of the various settings are given by Donnay and LePage[3]. Alpha-quartz and α - $A\ell PO_4$ are composed of 3-dimensional networks of MO_4 tetrahedra which may rotate under increased temperature to new positions, expanding the structure, and thus inducing a phase change to the hexagonal β-quartz structure (crystal class 622).

CRYSTAL GROWTH

Since α - $A\ell PO_4$ has an $\alpha \rightarrow \beta$ phase transition similar to quartz at 581°C, and is also unstable below 135°C in phosphoric acid, hydrothermal growth is a viable technique. Except for the fact that α - $A\ell PO_4$ has a retrograde solubility in H_3PO_4, standard quartz hydrothermal growth methods using steel autoclaves may be applied[4-7]. Crystals may be either nucleated spontaneously on the walls of the autoclave, or on oriented seed plates which are supported by platinum wires. However, no visual observation of in-situ growth can be routinely accomplished using these methods. Because of this restriction, considerable care must be exercised in both the preparation and process control of the growth run. However, hydrothermal techniques have been developed to grow α - $A\ell PO_4$ that would permit direct observation of crystal formation during free-nucleated and seeded growth[8,9]. In these methods, saturated solutions of $H_3PO_4/A\ell PO_4$ are sealed in quartz or demountable glass vessels and placed in standard laboratory ovens. An arrangement for direct line-of-sight or imaging optics would be required for visual observation. A third hydrothermal method uses the sealed quartz ampoule concept, but the ampoule is heated by a circulating, transparent silicone oil bath whose temperature can be precisely programmed. In this method several ampoules are placed in a single or double silicone oil bath using Pyrex® containers and are in full view. One can observe seed etch-back, nucleation and veil formation at the seed-crystal interface and in the bulk crystal. This allows, in a minimum number of runs, the determination of optimum growth conditions[10].

DEFECTS

Five different types of defects have been found in α - $A\ell PO_4$: twinning, crevicing, veiling, cracking, and surface etching. Except for twinning, the other defects can be alleviated by careful control and monitoring of the growth. Twinning and veiling are related to seed plate quality.

Twinning is common to α - $A\ell PO_4$ as well as to quartz. Both Dauphiné (electrical) and Brazil (optical) twinning occur in each. The axial and electrical relationships involved in both types of twinning singly, and in combination, are given in Figure 9. In optical

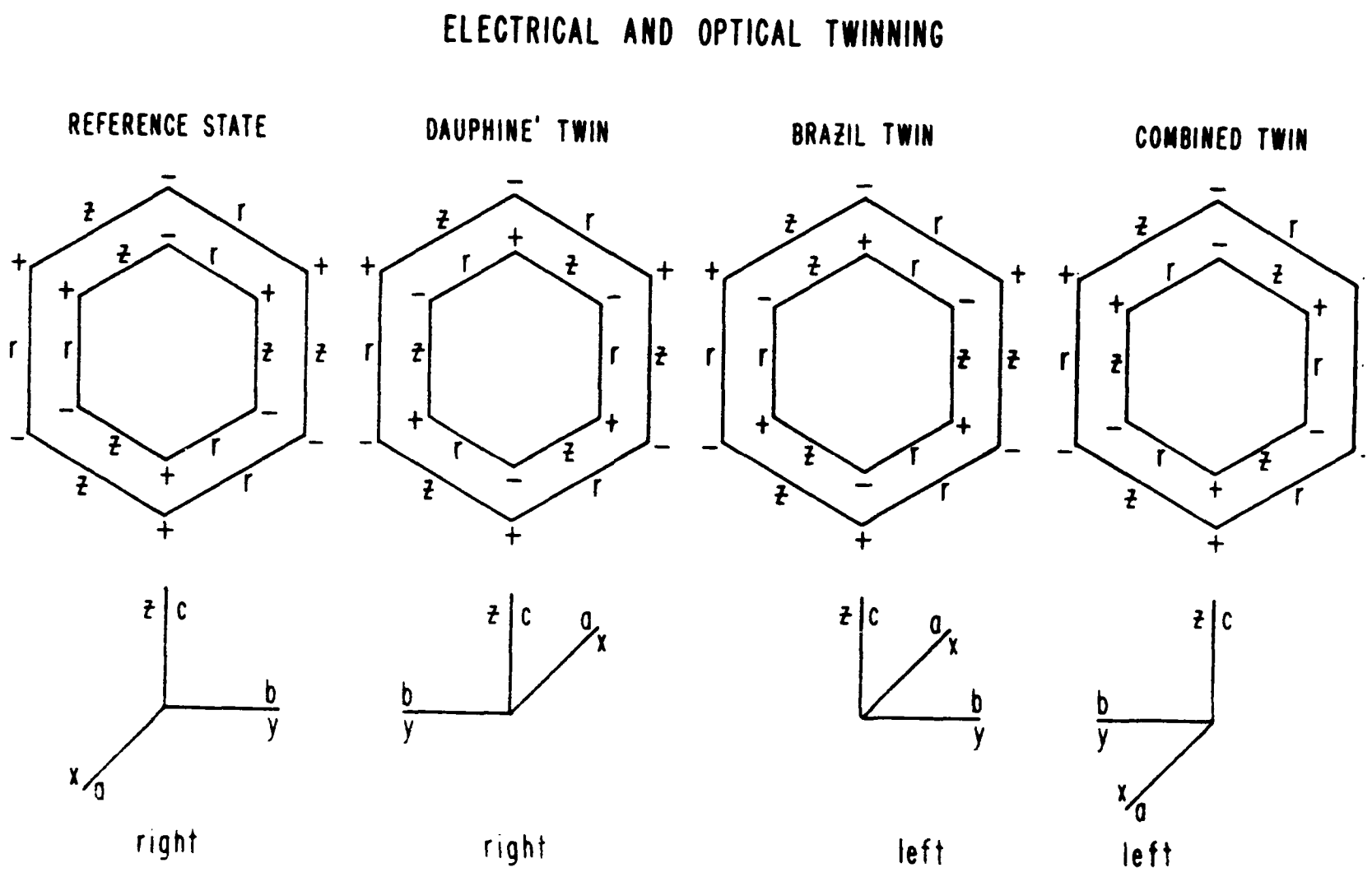

FIGURE 9. ELECTRICAL AND OPTICAL TWINNING

twinning, the domains of opposite handedness can be distinguished when the sample is viewed between crossed polarizers. In electrical twinning, the electrical polarity of the piezoelectric a axes in the twinned sections is reversed. Note in Figure 9 that in optical or Brazil twinning the electrical polarity is also reversed. The piezoelectric properties of a particular twinned sample could be radically altered. For example, in a piezoelectric crystal of class 32, the piezoelectric constant driving the pure shear mode of rotated-Y-cut plates is e'_{26}. This constant becomes modified by the type of twinning present, and, according to Table 2, a 50% fraction of Brazil twinning would reduce e'_{26}, and therefore the electromechanical coupling, to zero. Brazil twinning is very common in α - $A\ell PO_4$, while Dauphiné twinning is rarely observed. Both types are best detected by etching in saturated solutions of ammonium bifluoride. The twinning behavior of α - $A\ell PO_4$ is similar to that displayed by the amethyst variety of quartz. Amethyst almost always displays Brazil twinning and only rarely Dauphiné twinning.

TABLE 2 - ROTATED Y-CUT, PURE SHEAR MODE, CRYSTAL CLASS 32

TWINNING TYPE	e'_{26}
DAUPHINÉ	$T\ e_{11} \cos^2\theta - e_{14} \sin\theta \cos\theta$
BRAZIL	$T\ e_{11} \cos^2\theta + T\ e_{14} \sin\theta \cos\theta$
COMBINED	$-\ e_{11} \cos^2\theta + T\ e_{14} \sin\theta \cos\theta$
$T = (1-2A)$	A = Fraction of Active Area Twinned

Since Brazil twinning in amethyst is considered to be a consequence of the heavy iron impurity level[11], it is possible that Brazil twinning in α - $A\ell PO_4$ may also be impurity-induced.

THE H_2O IMPURITY

The dominant physical/chemical imperfection in α - $A\ell PO_4$ is undoubtedly the large H_2O content, as shown by infrared absorption in the 4000-2000 cm^{-1} region. Other impurities, for example the transition metal ions, are easily reduced to the limits of detectability by the crystallization process itself. One exception if Fe, which is, no doubt, related to the formation of ferric phosphates and mixed aluminum and ferric phosphates. The presence of water is possibly related to: (1) the growth process, i.e., the availability of H_2O through the reaction of H_3PO_4 with $A\ell PO_4$; (2) the fact that cavities sometimes occur in framework structures and may be occupied by replacable or irreplacable H_2O molecules; (3) the existence of compounds such as

variscite and metavariscite which have been shown to have the structure $A\ell\ PO_4 \cdot 2H_2O$ and have infrared absorption spectra remarkably similar to α - $A\ell\ PO_4$[12].

In the case of quartz, the correlation of material Q and infrared absorption due to OH in the neighborhood of 3500 cm^{-1} is well established. The IR transmission of α - $A\ell\ PO_4$ was measured in the 4000 to 2000 cm^{-1} region with a Perkin-Elmer Model 21 spectrophotometer. Figure 10 compares the IR transmittances of α-quartz and α-berlinite. Quartz samples must be at least 1 cm thick to record any absorption, while α - $A\ell\ PO_4$ must be thinned to at least 250μm because of the intense absorption in this region. The presence of a large amount of hydrogen is indicated.

Using formulas developed for quartz[13], we obtain an absorption coefficient at 3410 cm^{-1} from the expression

$$\alpha(3410) = (1/t) \cdot \log_{10} [T(3800)/T(3410)] = 20\ cm^{-1},$$

where t is thickness and T is transmission. The hydrogen concentration may be found from

$$N_H = 2.16 \times 10^{16}\ H\ \alpha(3410) = 1400 \times 10^{-6},$$

where H is the half-width of the peak absorption line. By contrast, using electron paramagnetic resonance (EPR) techniques, which are only sensitive to the presence of hydrogen atoms,

$$N_H = 75 \times 10^{-6}\ \text{(Reference 14)}.$$

This large difference suggests that most of the hydrogen could be present as water molecules. Recently, Shand and Chai[15] have confirmed the existence of large amounts of water in berlinite using Raman scattering spectroscopy (RSS). Again, using a formula developed for quartz[16], the infrared Q may be found from

$$Q \simeq 1.69 \times 10^5/\alpha(3410) = 8{,}500.$$

RESONATORS

Frequency constants, piezoelectric coupling factors, and temperature coefficients of frequency for the plate thickness modes have been computed for doubly rotated[17] cuts of berlinite based on the measurements of Chang and Barsch[19]. For the doubly rotated orientations shown in (b) of Figure 1, having the orientational notation $(YXw\ell)\ \phi/\theta$ the frequency constants N_m (in MHz-mm) of the three thickness plate modes are given in Figure 11 to Figure 16 for $\phi = 0^0\ (6^0)\ 30^0$ and $|\theta| \leq 90^0$. The modes m = a, b, and c denote, respectively, the quasilongitudinal, fast quasishear, and slow quasishear modes in the plate thickness direction. In Figure 17 to Figure 22 are given the corresponding curves of piezoelectric coupling |k|. Figure 23 to

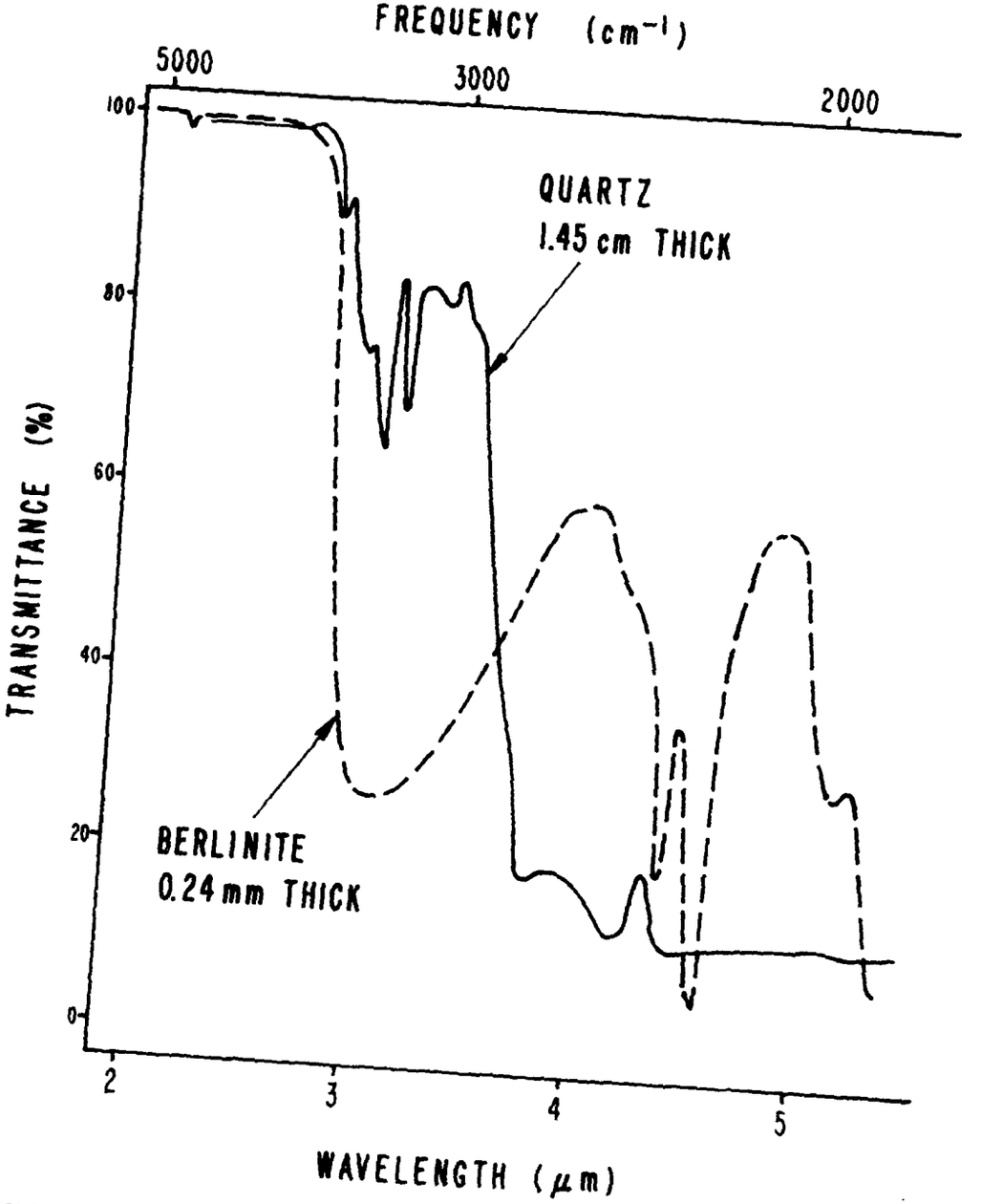

FIGURE 10. IR TRANSMITTANCE OF QUARTZ AND BERLINITE

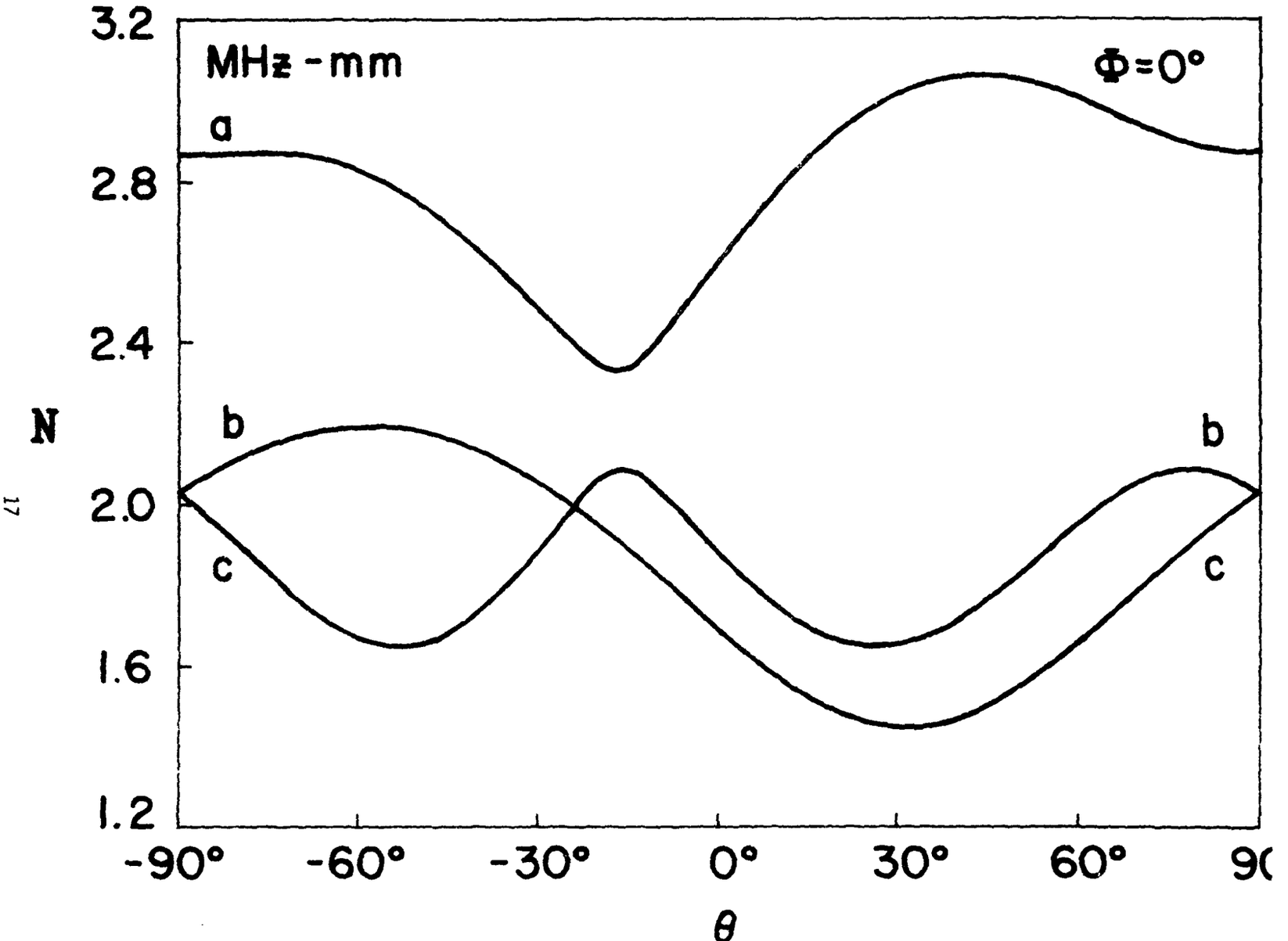

FIGURE 11. FREQUENCY CONSTANTS OF (YXwℓ) 0°/θ BERLINITE

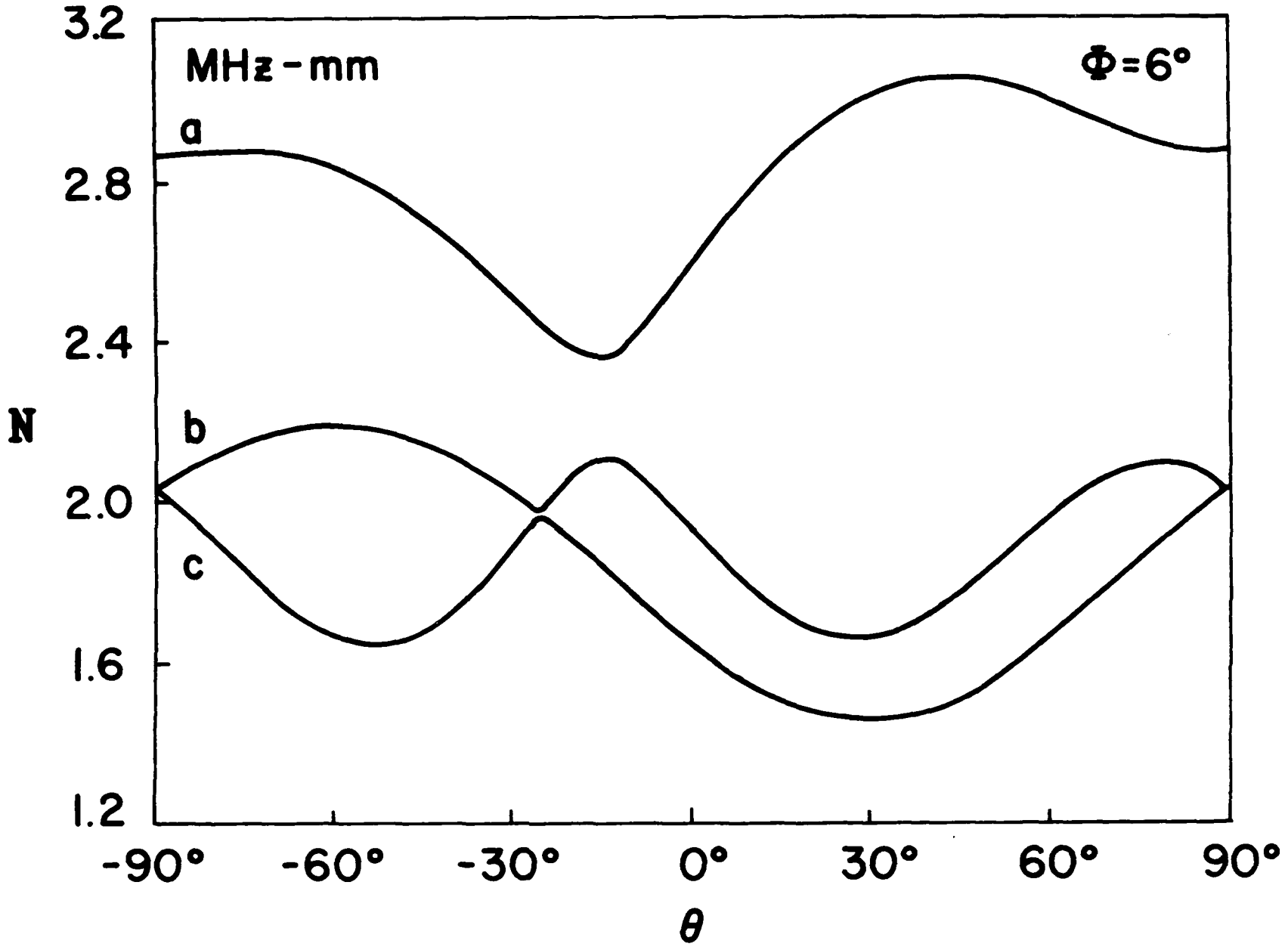

FIGURE 12. FREQUENCY CONSTANTS OF (YXwℓ) 6°/θ BERLINITE

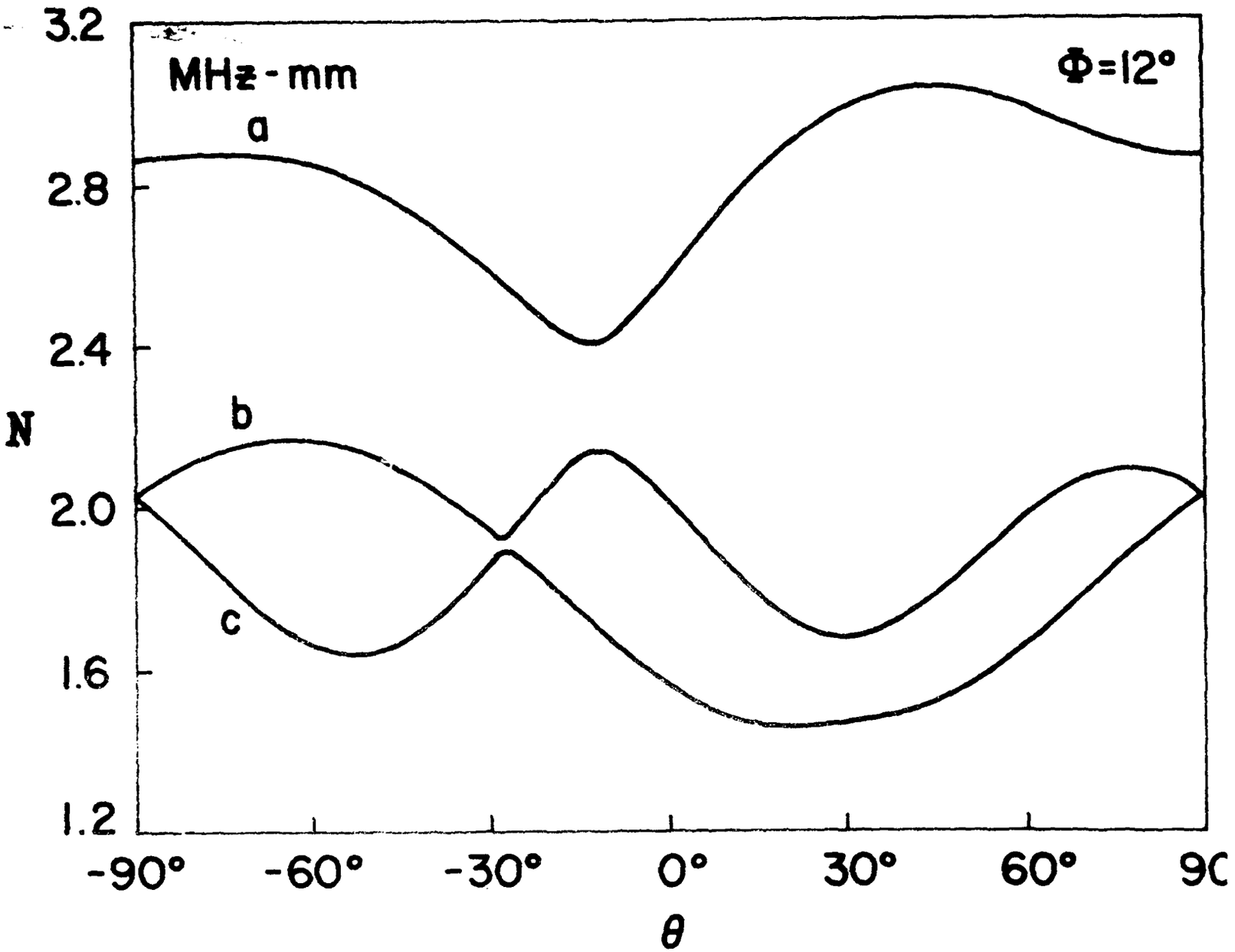

FIGURE 13. FREQUENCY CONSTANTS OF (YXwℓ) 12°/e BERLINITE

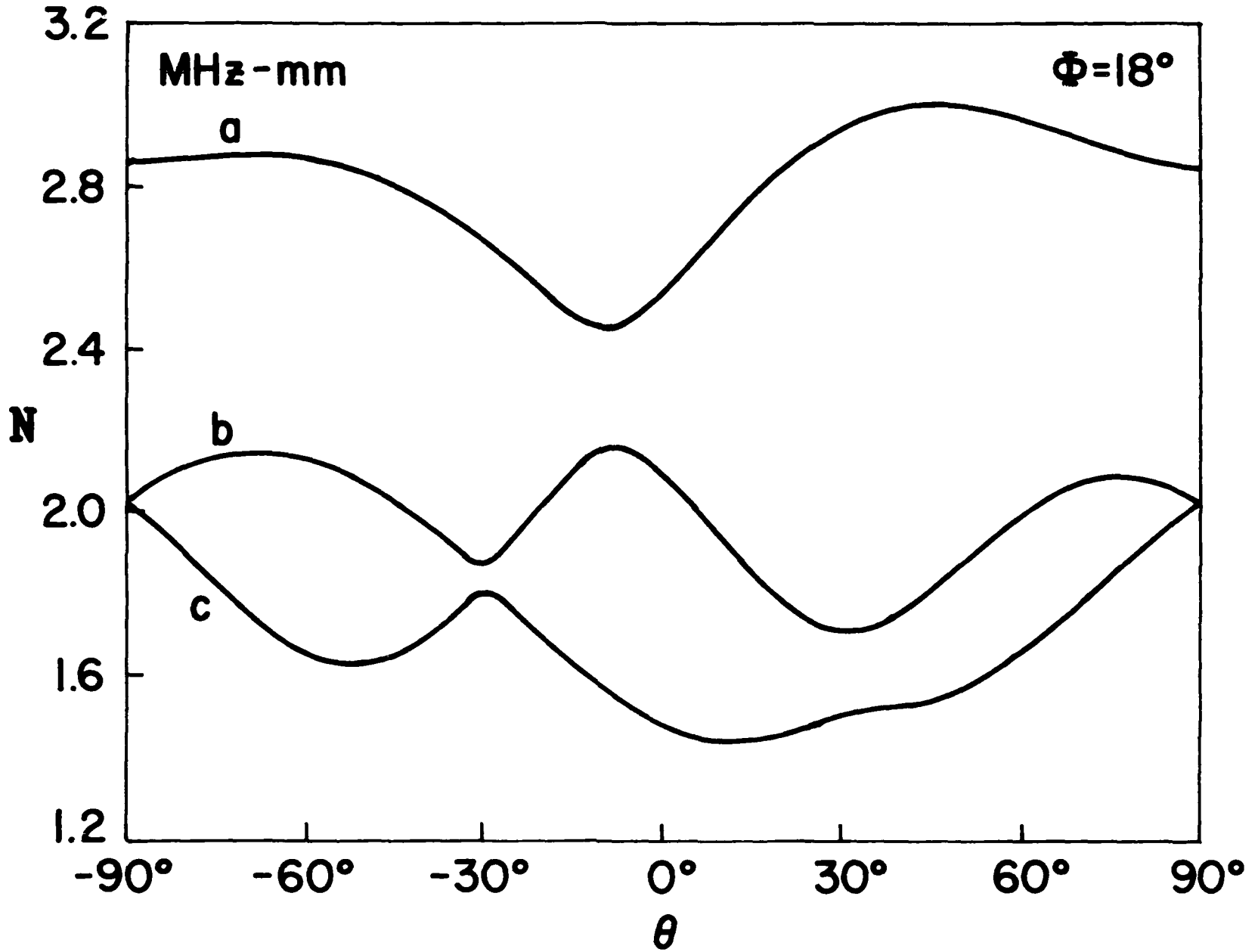

FIGURE 14. FREQUENCY CONSTANTS OF (YXwℓ) 18°/θ BERLINITE

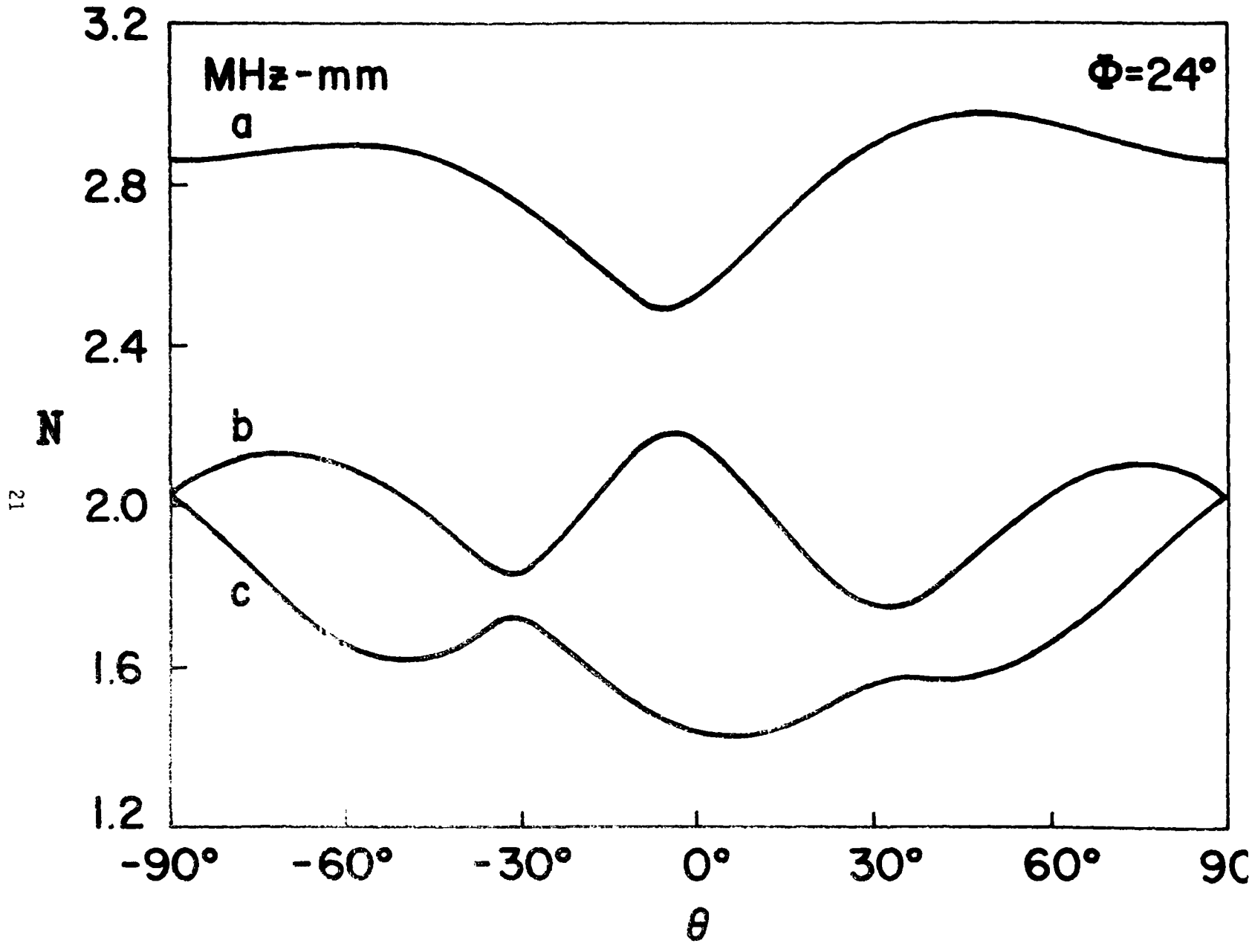

FIGURE 15. FREQUENCY CONSTANTS OF (YXw:ℓ) 24°/θ BERLINITE

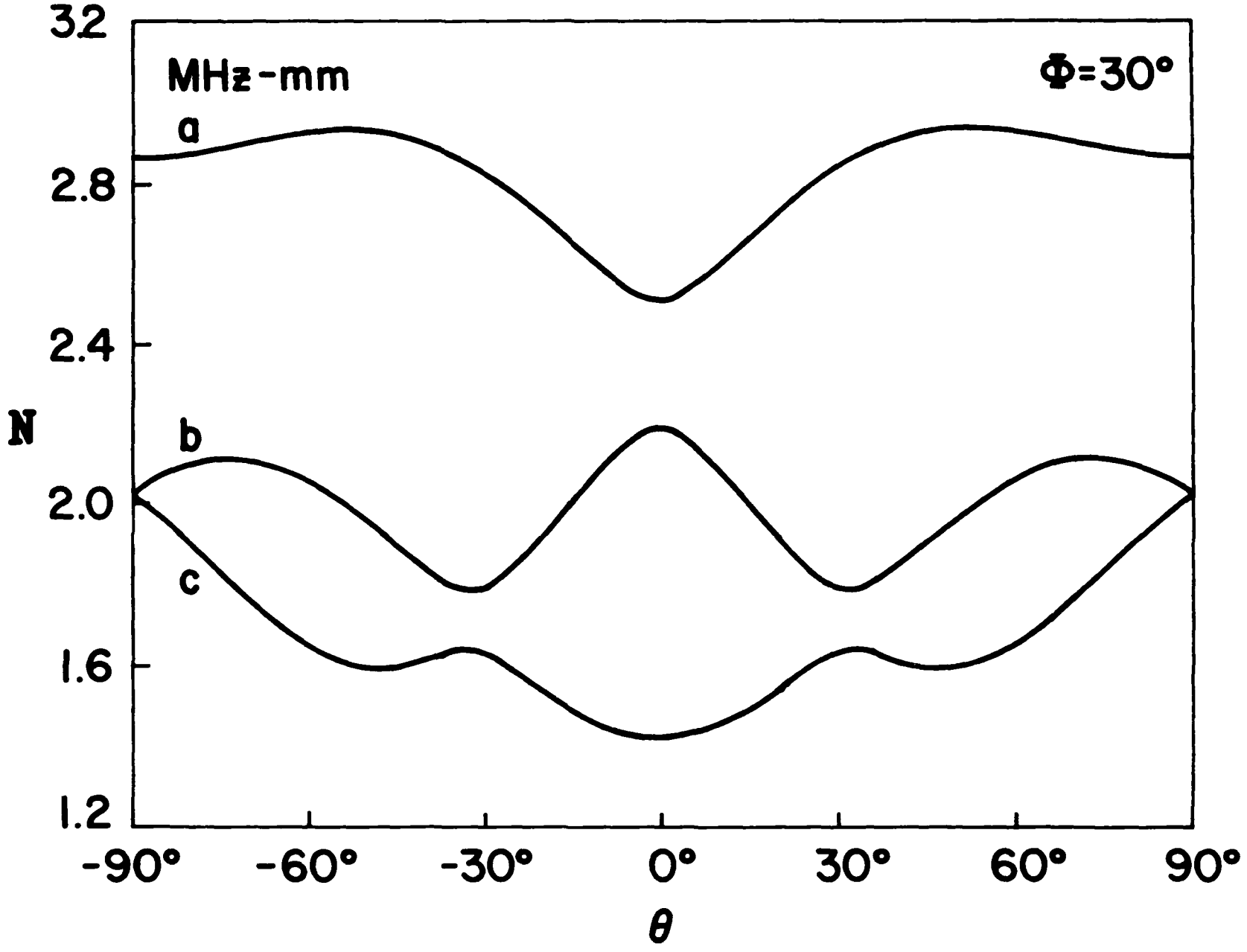

FIGURE 16. FREQUENCY CONSTANTS OF (YXwℓ) 30°/θ BERLINITE

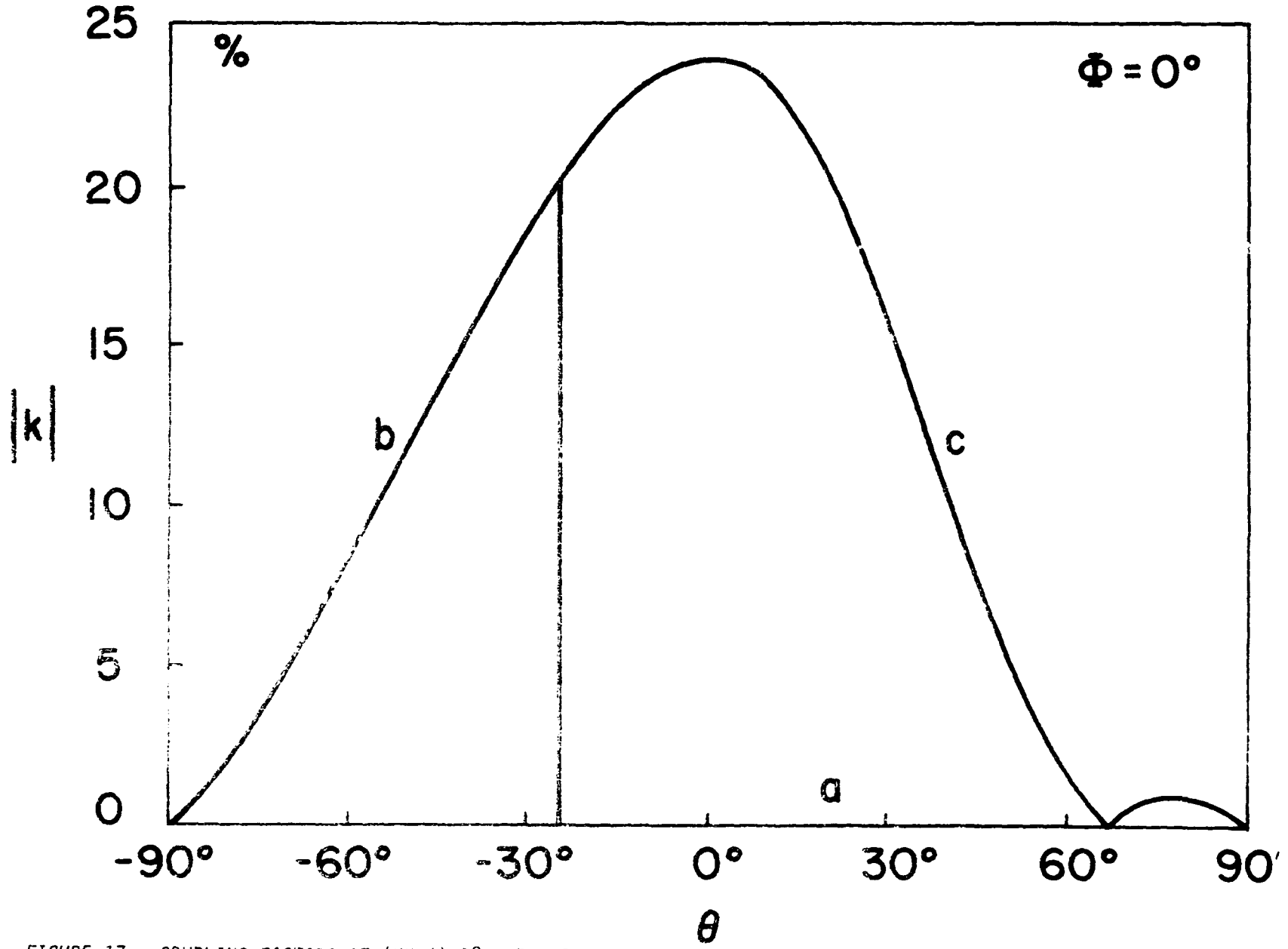

FIGURE 17. COUPLING FACTORS OF (YXwℓ) 0°/6 BERLINITE

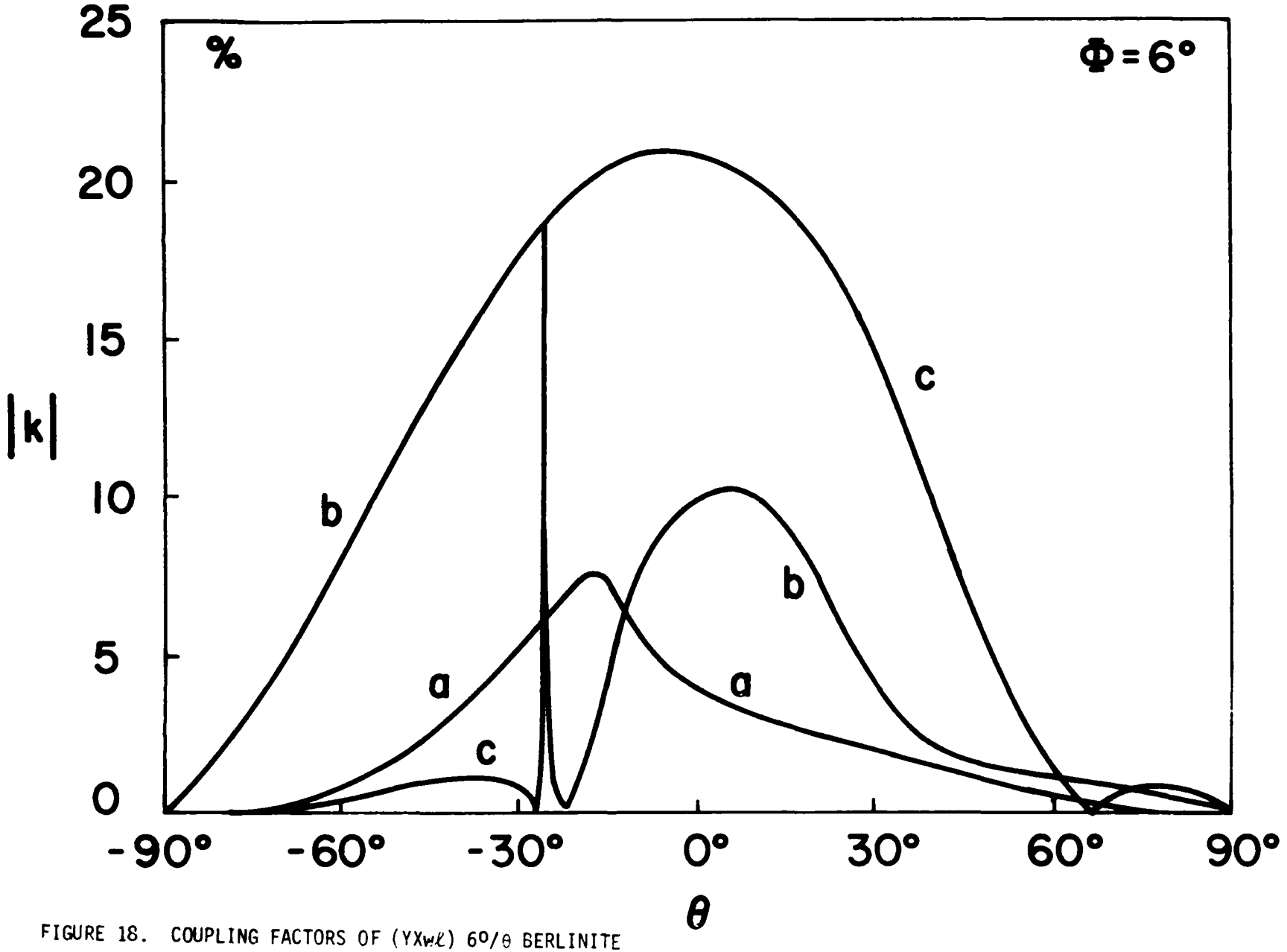

FIGURE 18. COUPLING FACTORS OF (YXwℓ) 6°/θ BERLINITE

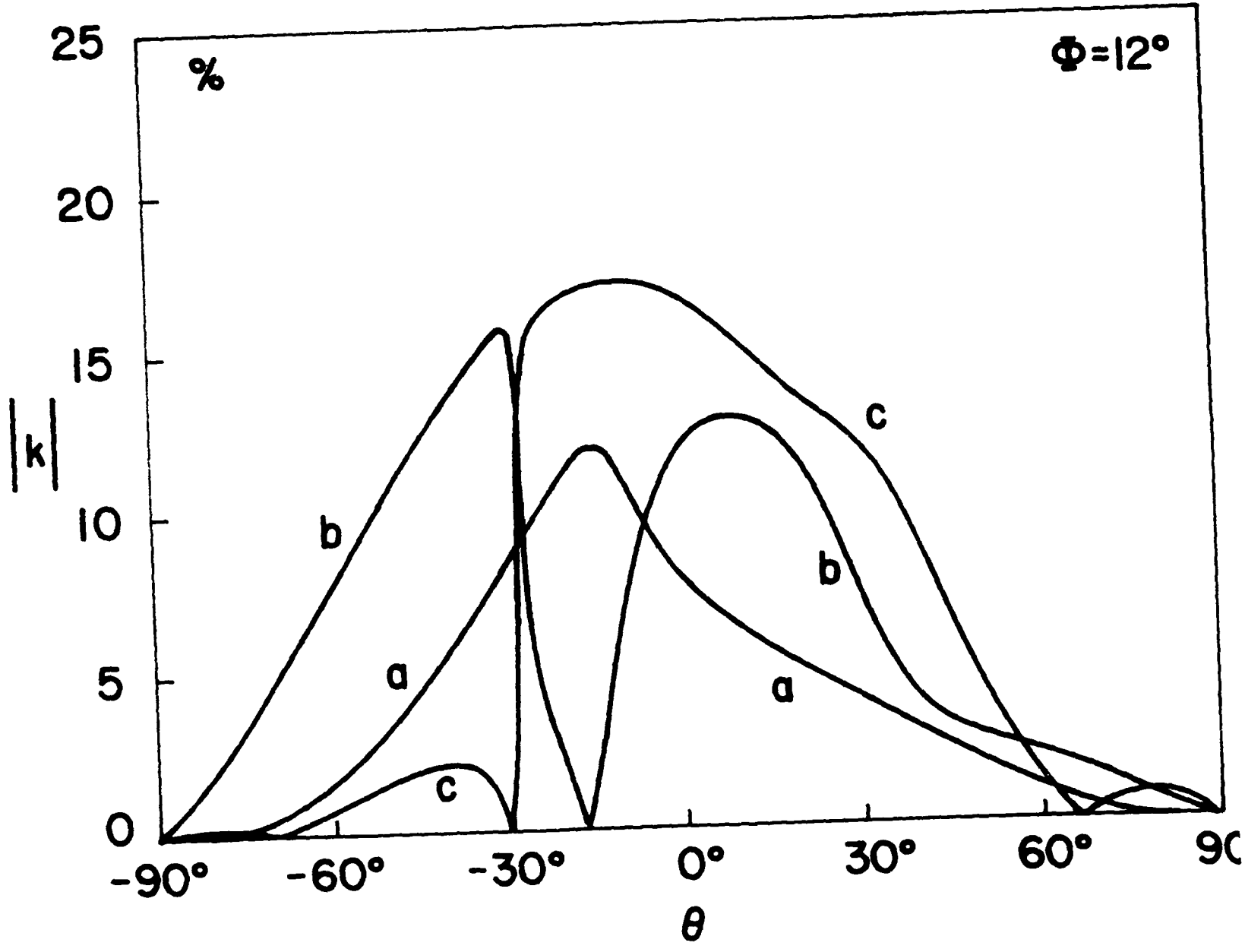

FIGURE 19. COUPLING FACTORS OF (YXwℓ) 12°/θ BERLINITE

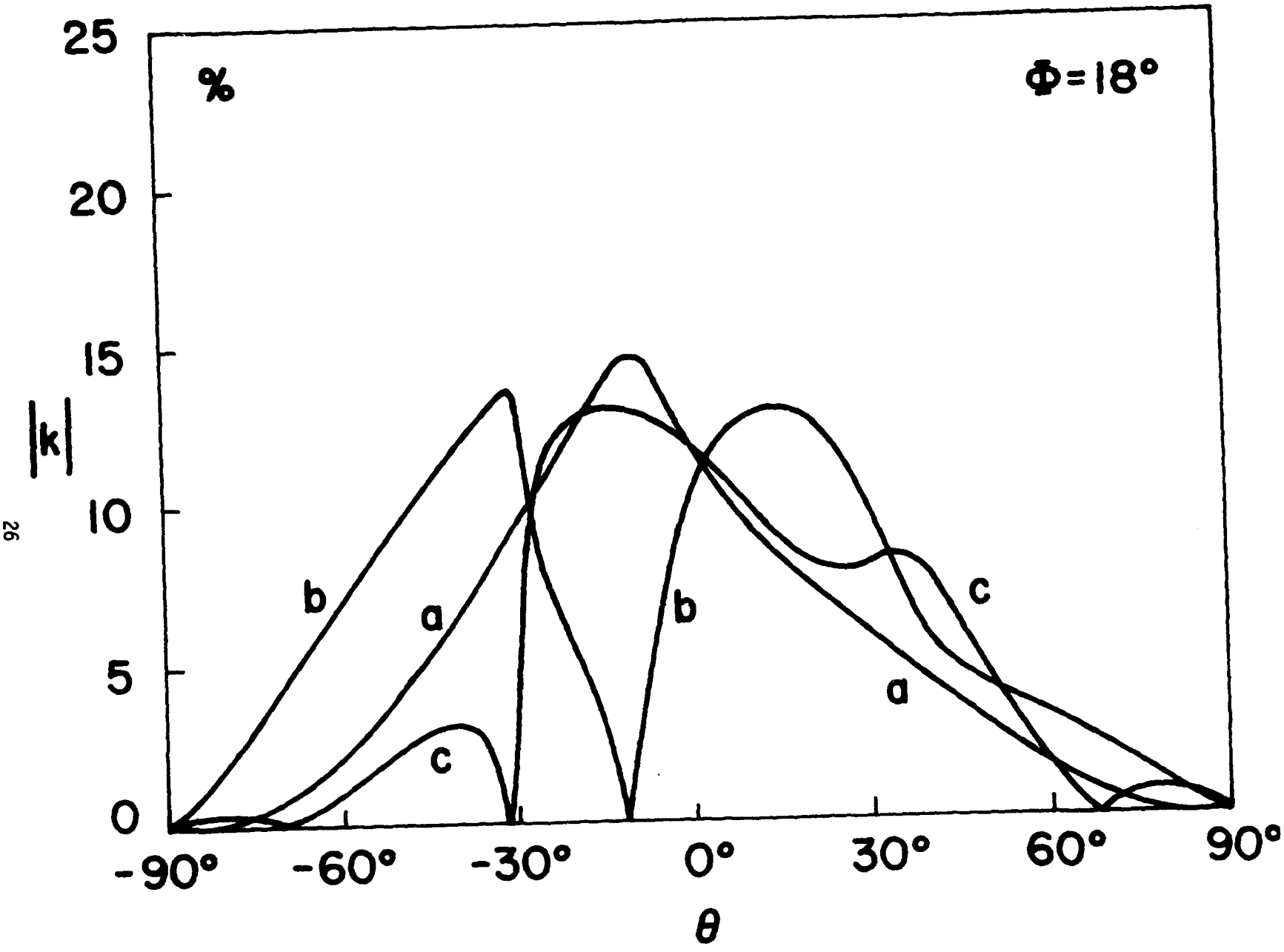

FIGURE 20. COUPLING FACTORS OF (YXwℓ) 18°/θ BERLINITE

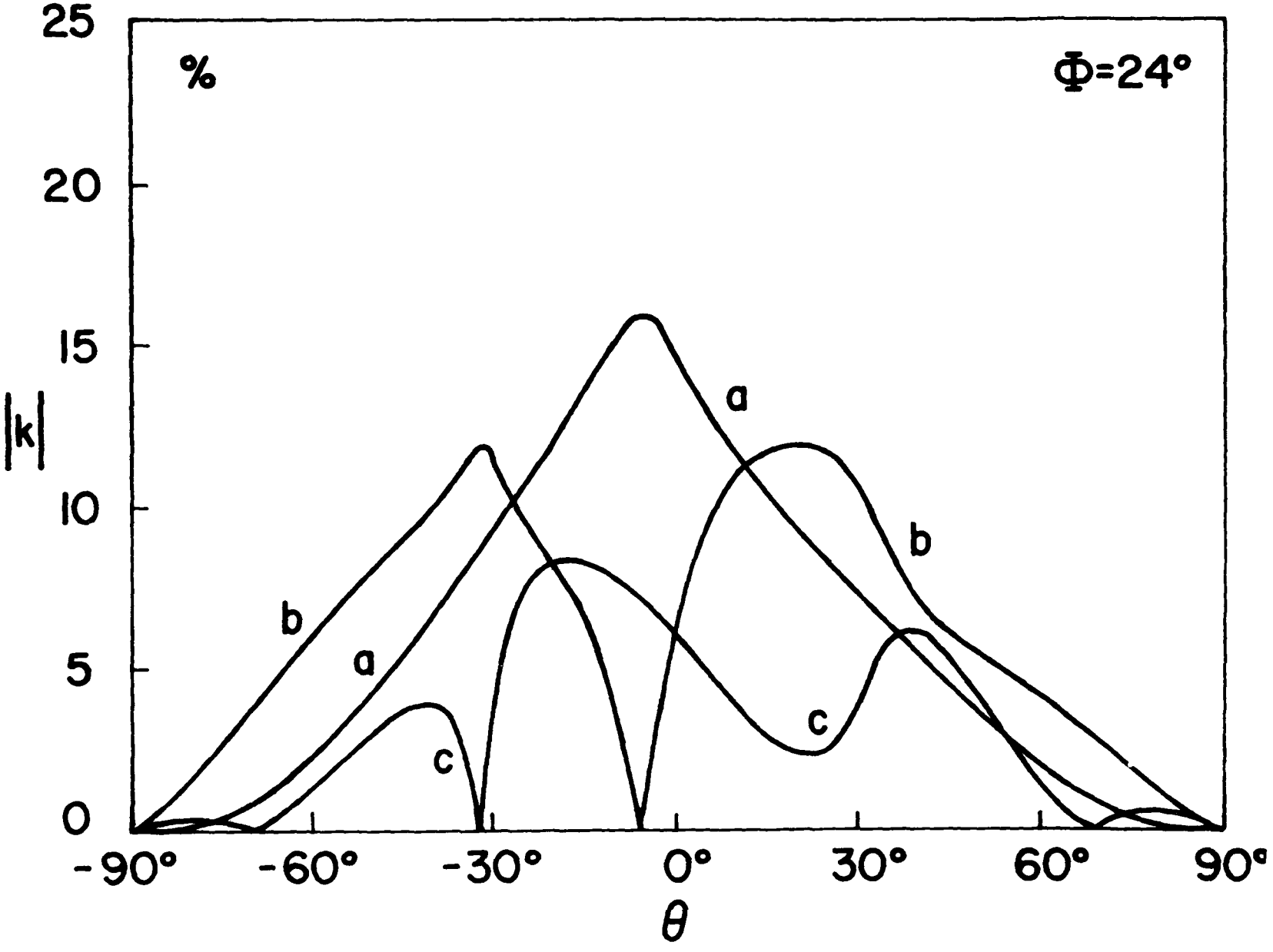

FIGURE 21. COUPLING FACTORS OF (YXwℓ) 24°/θ BERLINITE

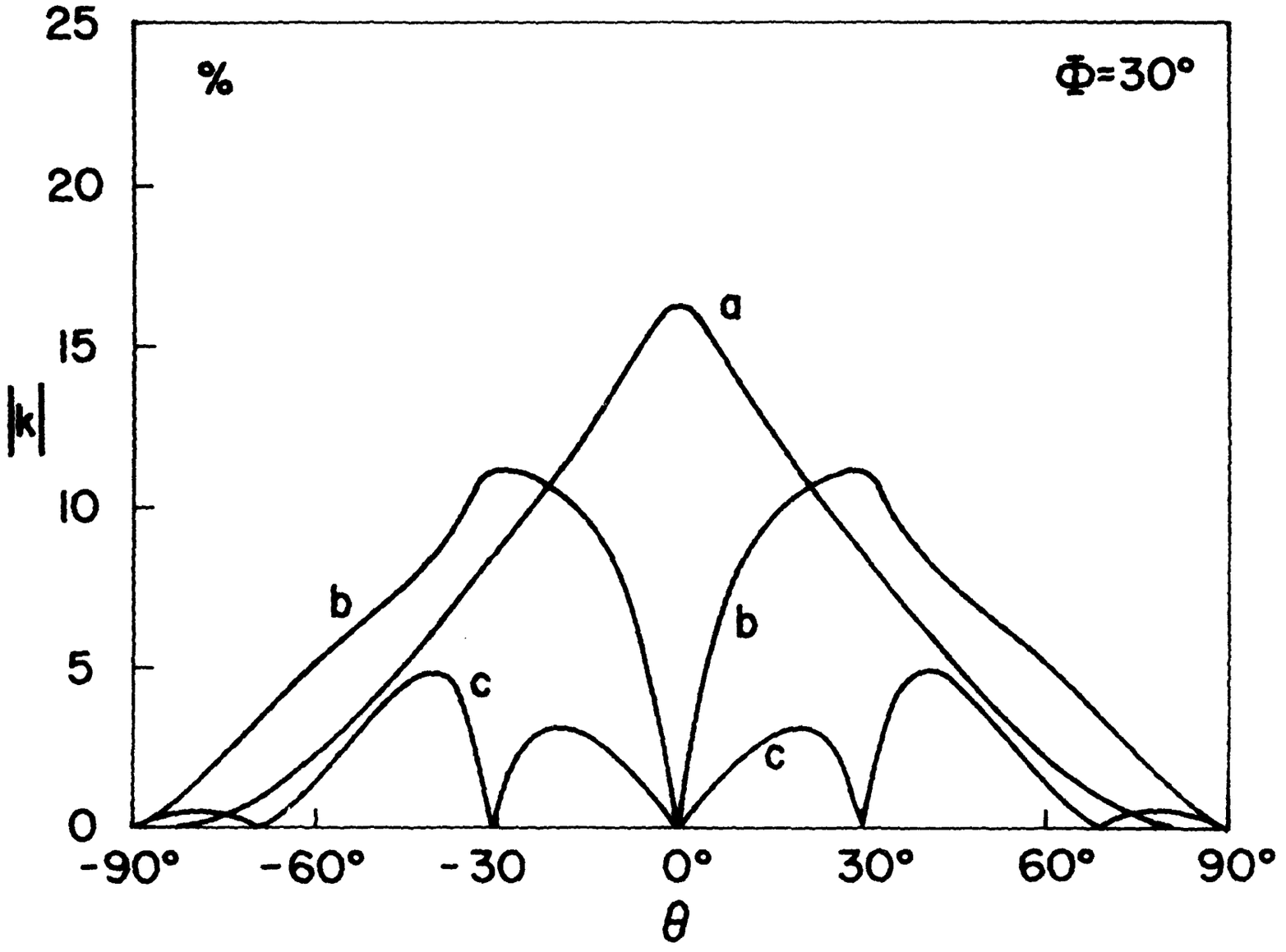

FIGURE 22. COUPLING FACTORS OF (YXwℓ) 30°/θ BERLINITE

Figure 28 display the linear temperature coefficient of frequency T_{f_a} of these three modes.

The loci of zeros of first-order temperature coefficient of antiresonance frequency as a function of ϕ and θ have also been determined, and are shown in Figure 29.

The frequency constants N_m and coupling factors $|k|$ are given in Figure 30 and Figure 31, respectively, for the thickness modes a, b, and c of berlinite plates having orientations $(YXw)\phi$.

Table 3 gives the values of N_m and $|k_m|$ for both X-cut ($\theta=0^o$, $\phi=30^o$) and Y-cut ($\theta=0^o$, $\phi=0^o$) α - $A\ell PO_4$. The "c" mode linear temperature

TABLE 3 - FREQUENCY CONSTANTS AND COUPLING FACTORS OF THE THICKNESS MODES OF X- AND Y-CUT BERLINITE

MODE	N_m MHz-mm	$\|k_m\|$ percent	CUT
a	2.50	16.2	X
b	2.19	0	X
c	1.43	0	X
a	2.58	0	Y
b	1.89	0	Y
c	1.70	24.0	Y

coefficient of frequency for cuts $(YXw)\phi$ monotonically decreases from $+40 \times 10^{-6}/K$ at the Y-cut, to zero at the X-cut: for the "b" mode the corresponding values are $-95 \times 10^{-6}/K$, increasing monotonically to $-30 \times 10^{-6}/K$.

An $A\ell PO_4$ crystal plate was cut from an as-grown specimen close to a major rhombohedral face $(YX\ell)$ $\theta \approx 50^o$. The plate thickness was 0.31 mm and the fundamental resonance frequency was 5 MHz. The resulting mode spectrum is shown in Figure 32. Other resonances were found out to the 13th harmonic at 65 MHz. In the measurement, the sample was placed in a special air-gap holder[20]. A block diagram of the various components associated with this measurement is shown in Figure 33.

THE EQUIVALENT CIRCUIT

The equivalent electrical circuit for a piezoelectric plate vibrator in the vicinity of a single resonance is shown in Figure 34. The circuit element values are expressible in terms of the material

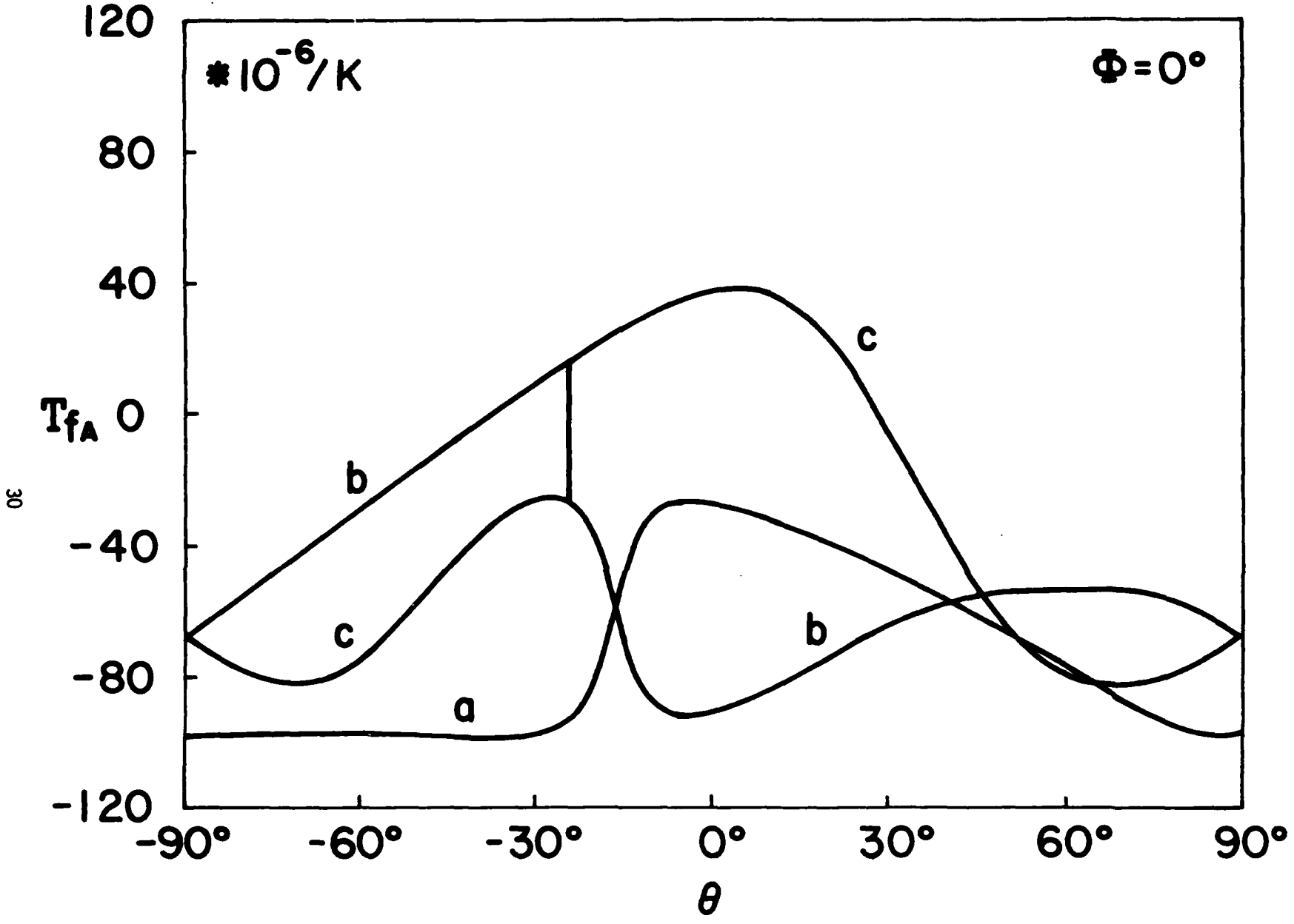

FIGURE 23. TEMPERATURE COEFFICIENTS OF (YXwℓ) 0°/θ BERLINITE

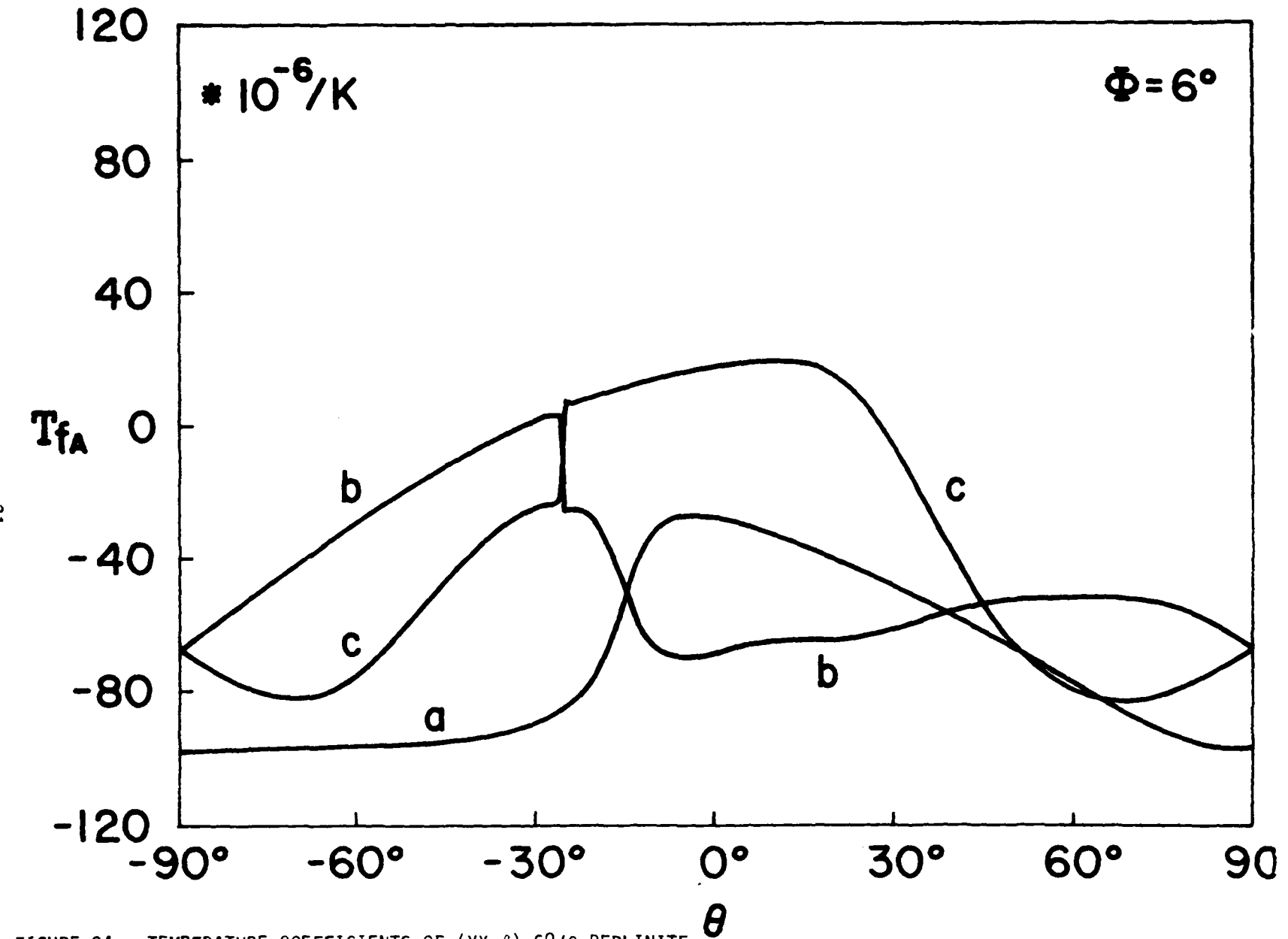

FIGURE 24. TEMPERATURE COEFFICIENTS OF (YXwℓ) 6°/θ BERLINITE

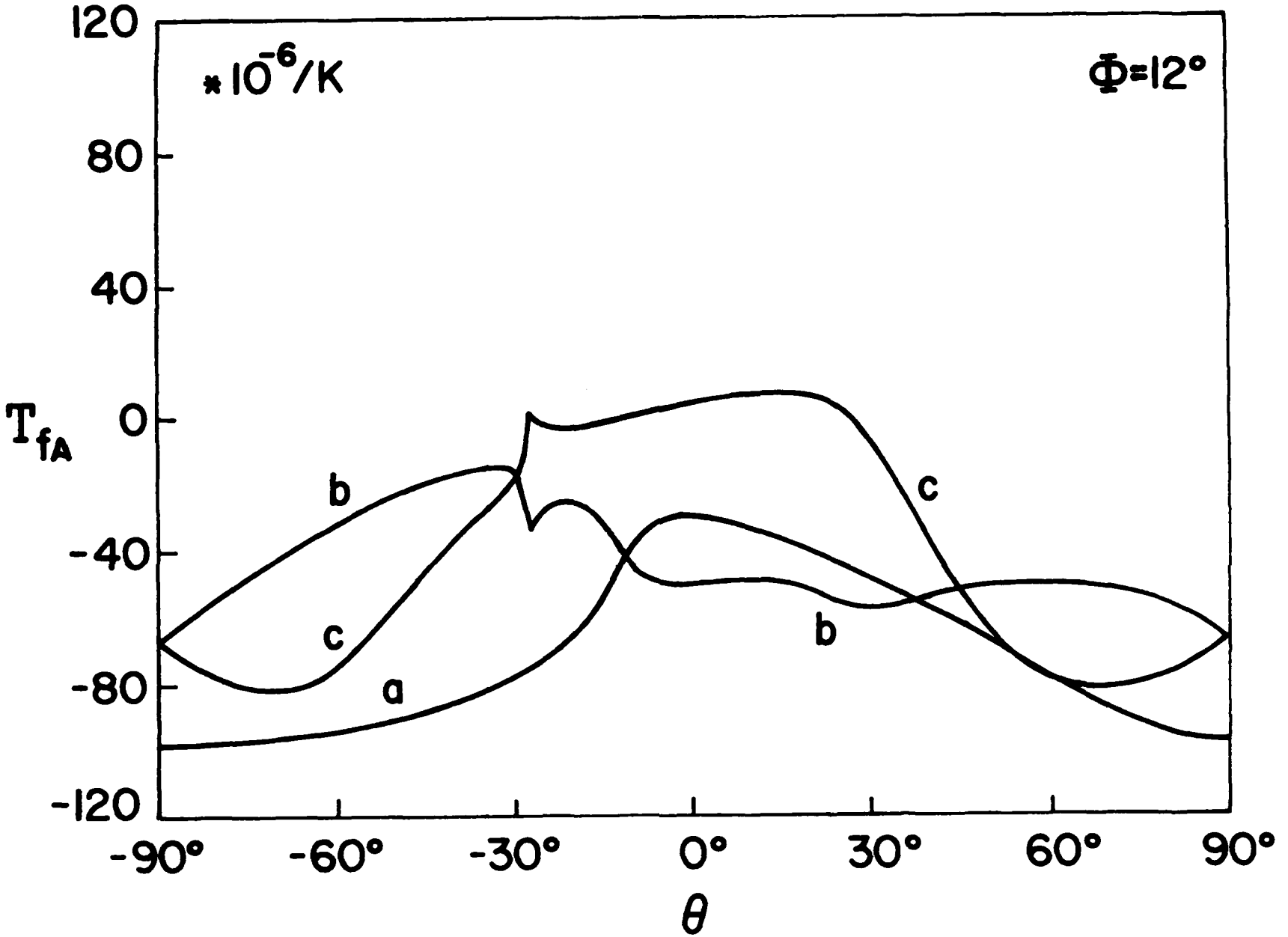

FIGURE 25. TEMPERATURE COEFFICIENTS OF (YXwℓ) 12°/θ BERLINITE

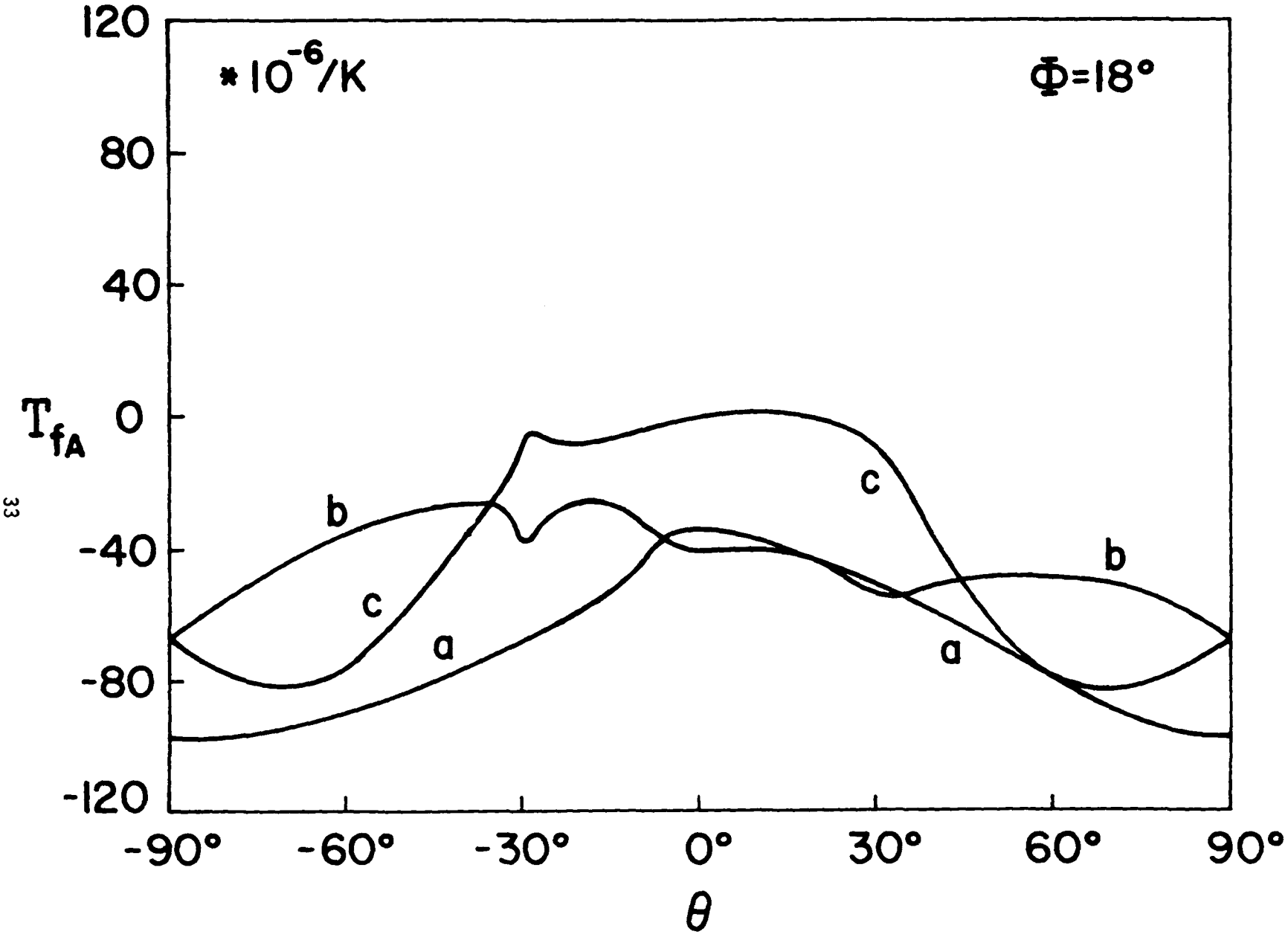

FIGURE 26. TEMPERATURE COEFFICIENTS OF (YXwℓ) 18°/θ BERLINITE

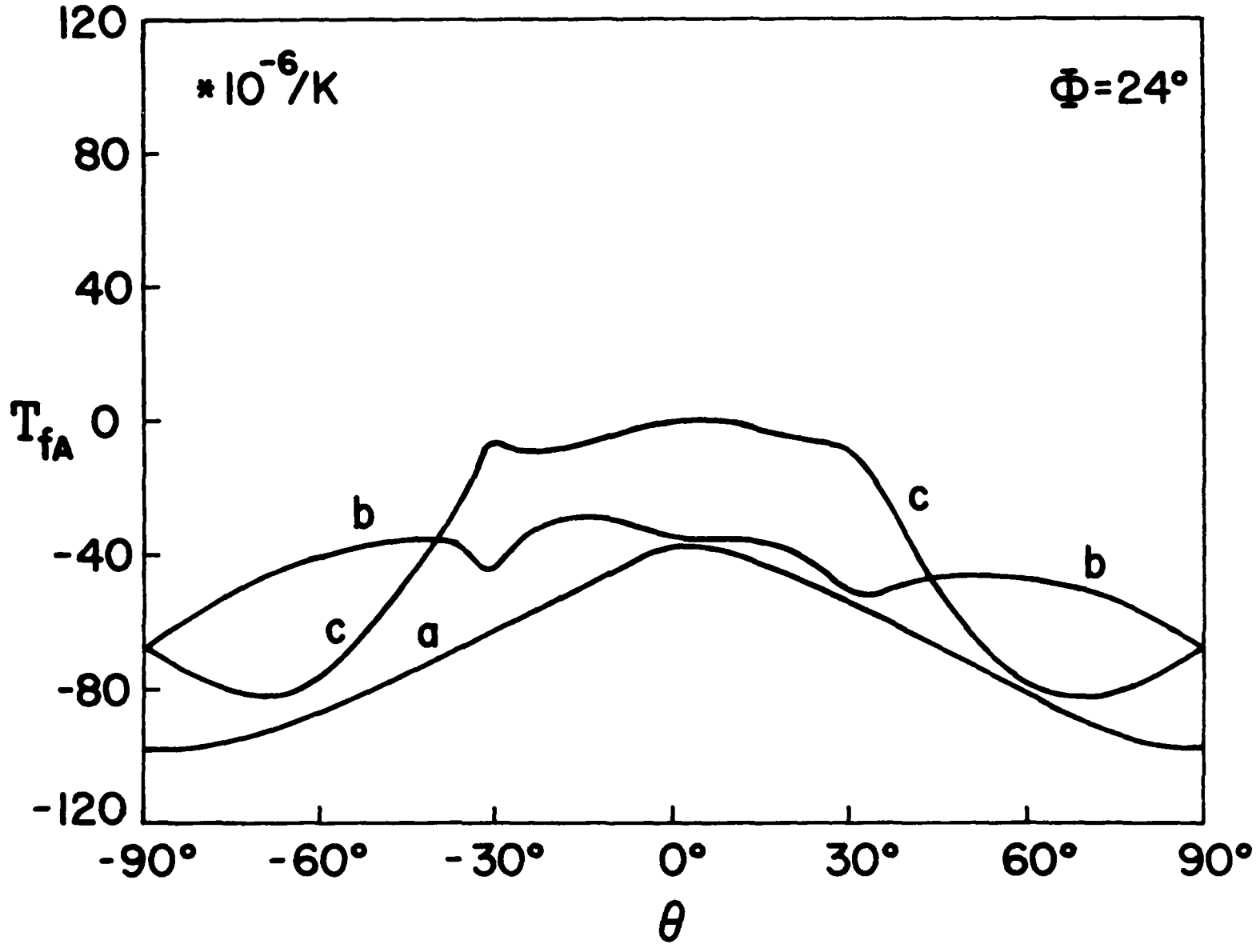

FIGURE 27. TEMPERATURE COEFFICIENTS OF (YXwℓ) 24°/θ BERLINITE

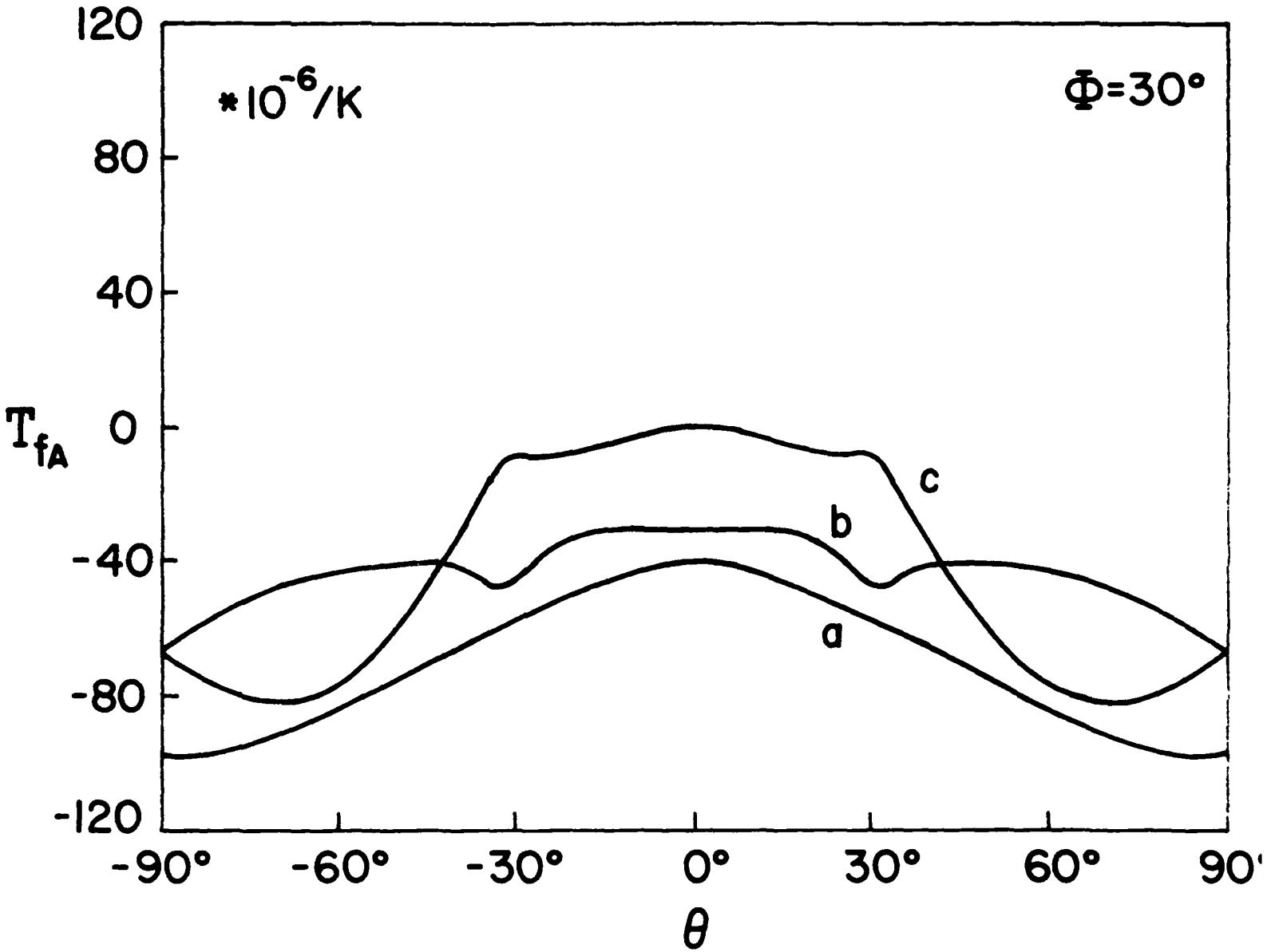

FIGURE 28. TEMPERATURE COEFFICIENTS OF (YXwℓ) 30°/e BERLINITE

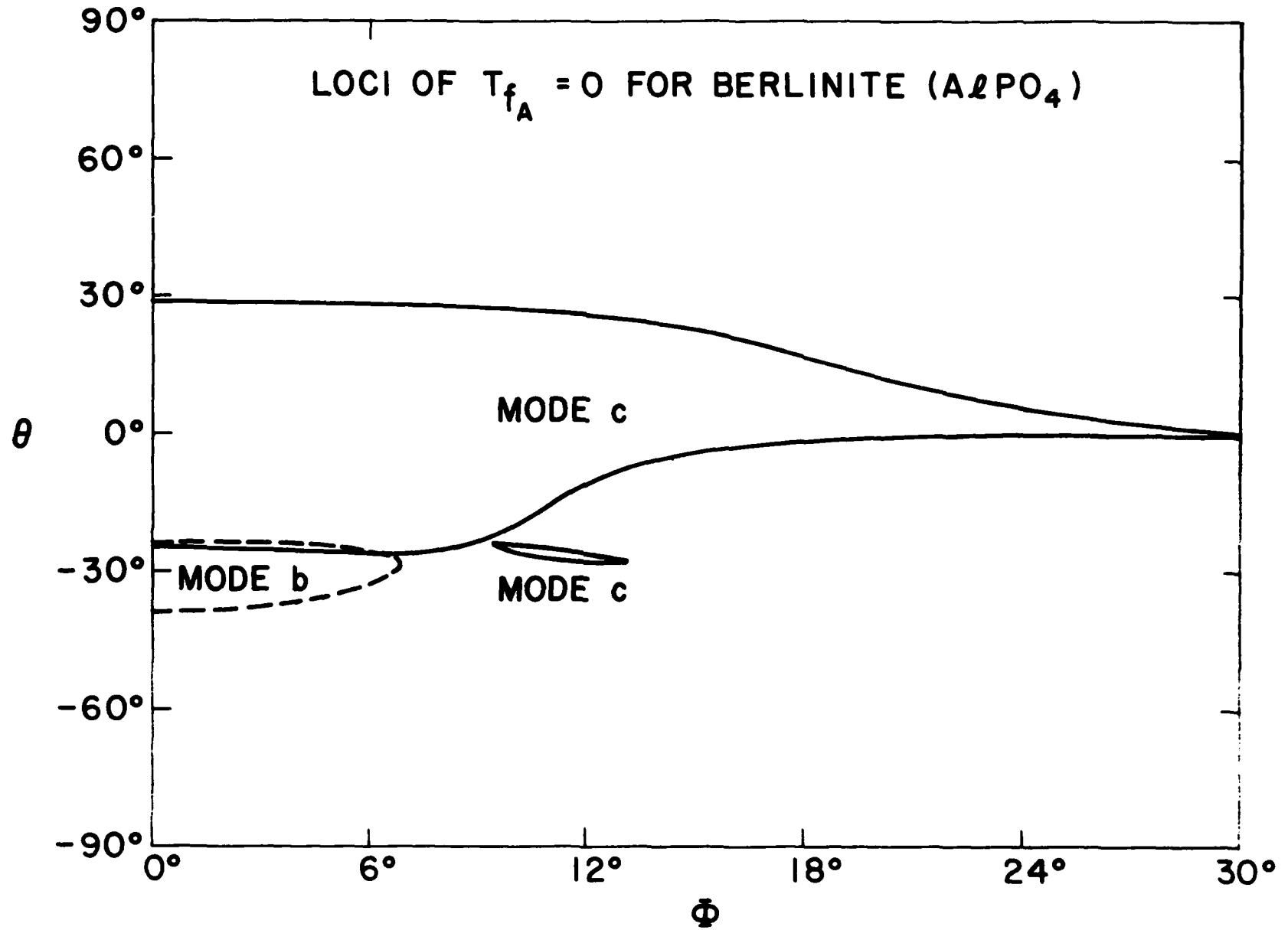

FIGURE 29. LOCI OF ZERO TEMPERATURE COEFFICIENT FOR BERLINITE

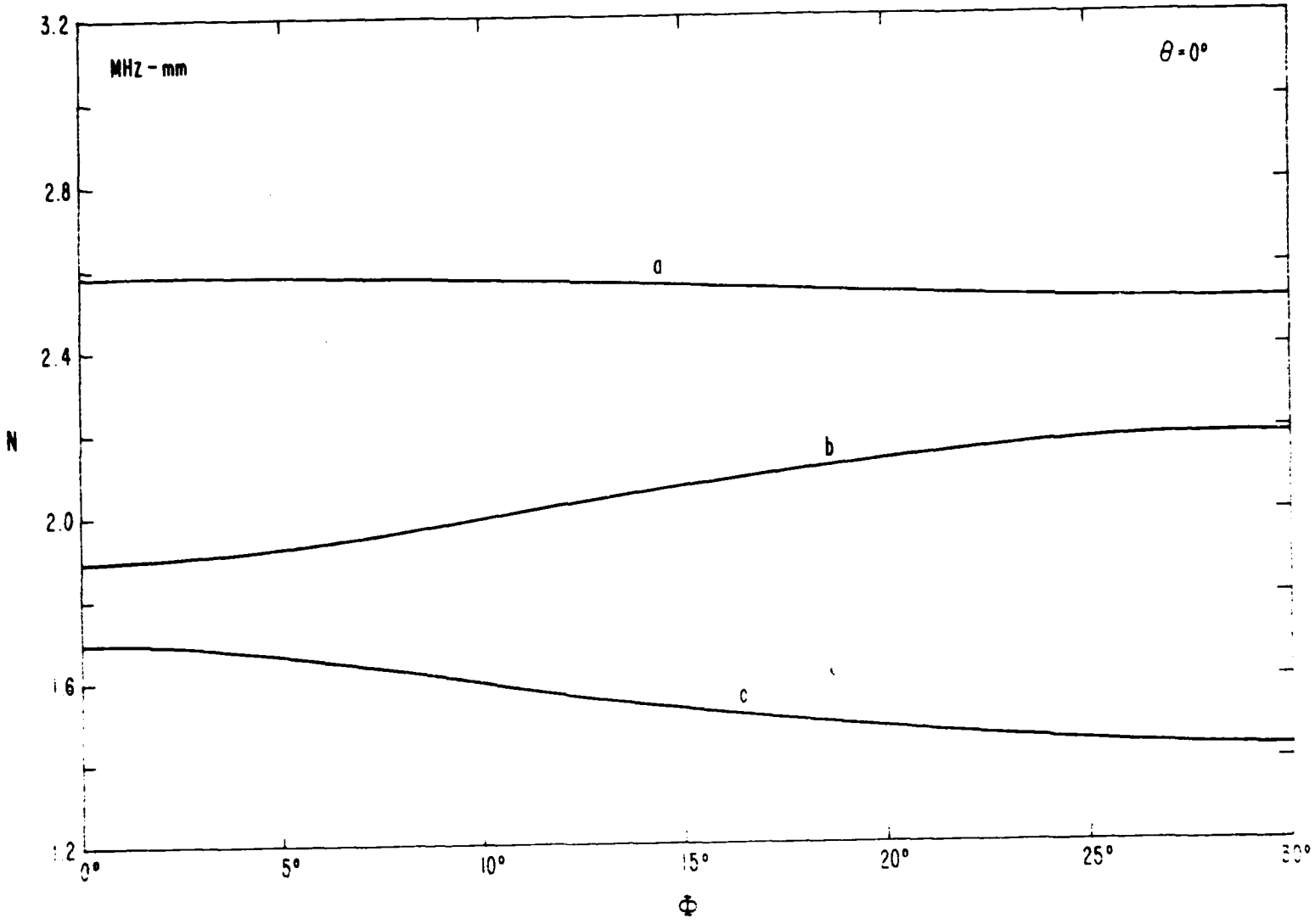

FIGURE 30. FREQUENCY CONSTANTS FOR (YXw)ϕ BERLINITE

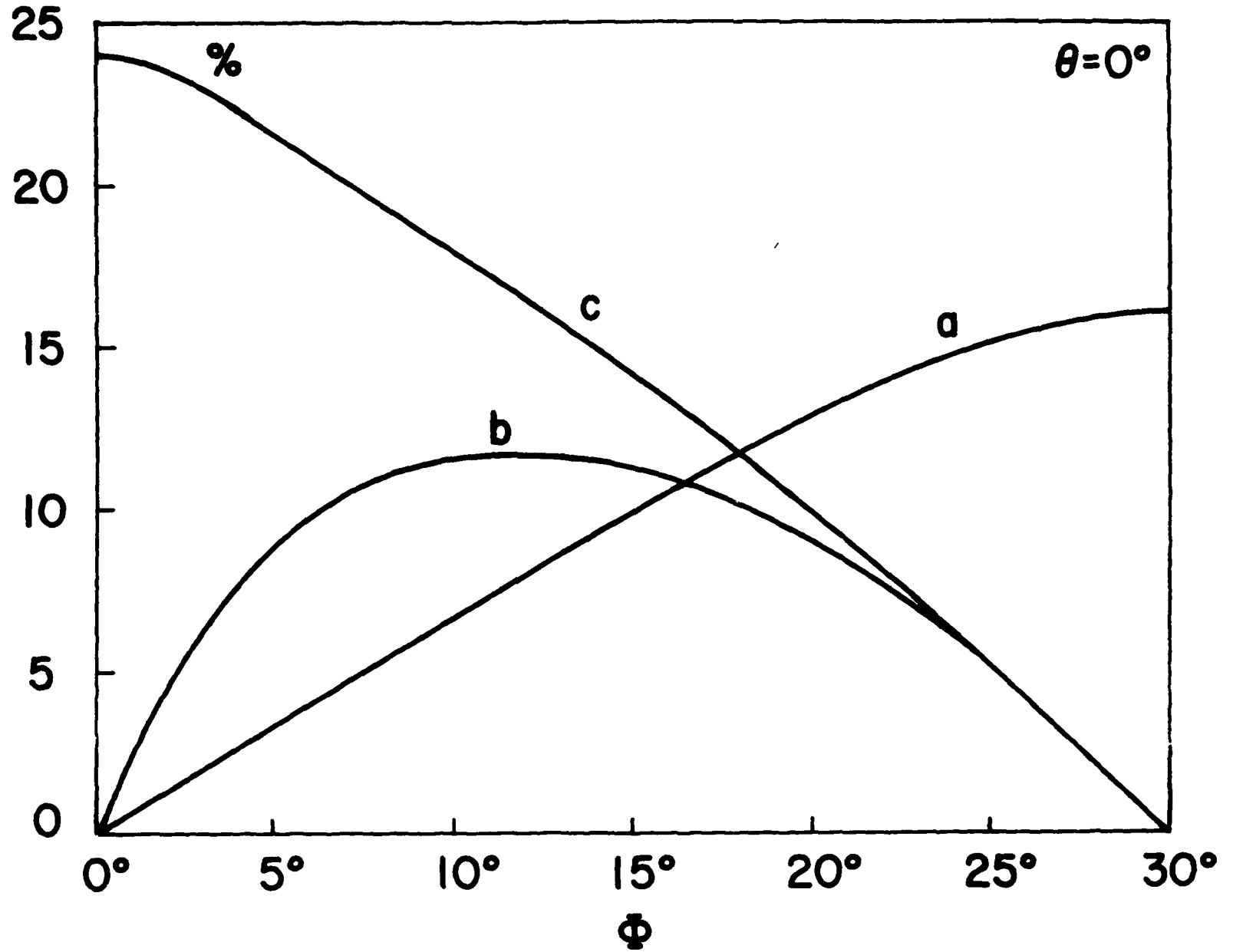

FIGURE 31. COUPLING FACTORS FOR (YXw)c BERLINITE

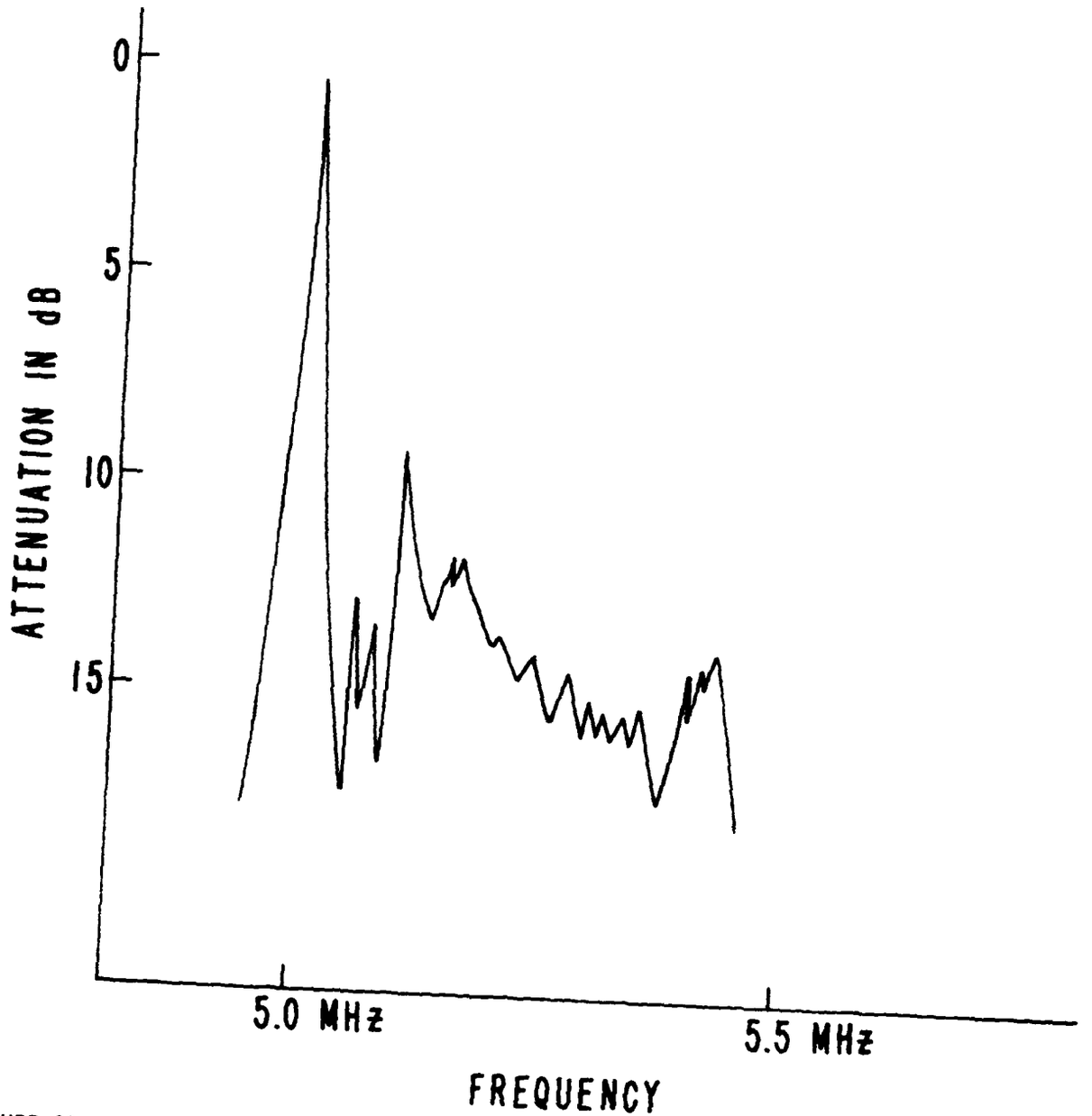

FIGURE 32. MODE SPECTROGRAPH OF BERLINITE RESONANCE

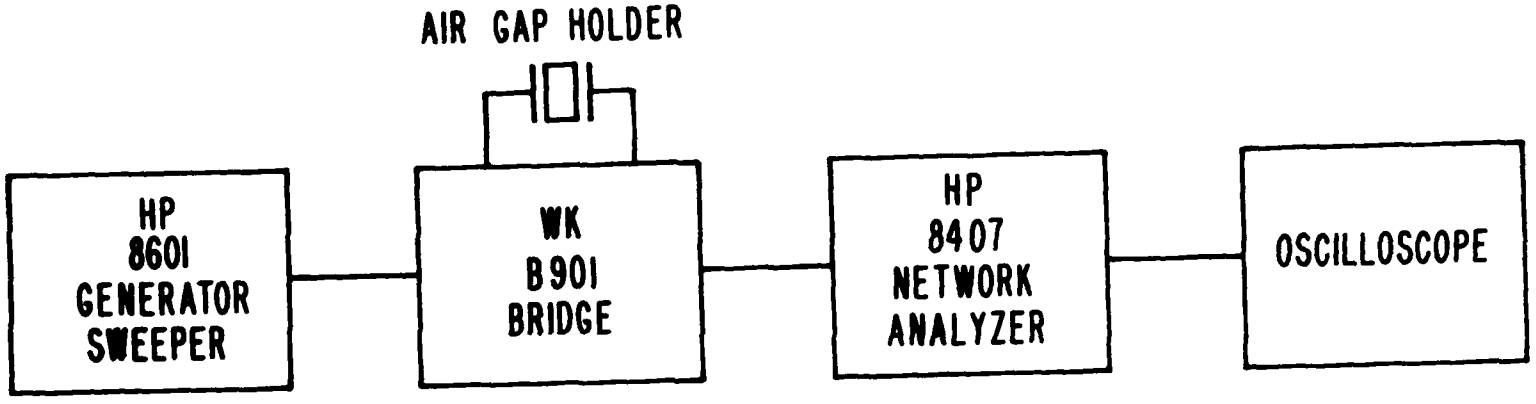

FIGURE 33. BLOCK DIAGRAM OF MEASUREMENT

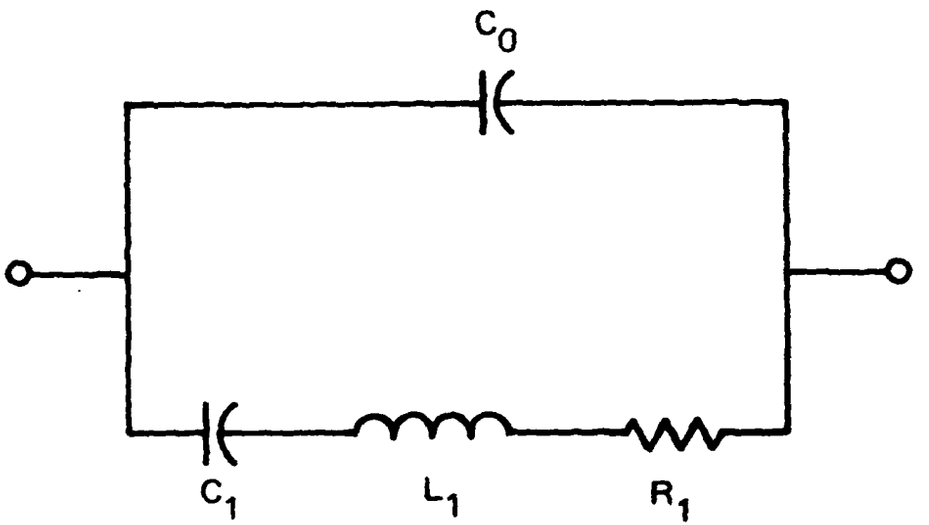

FIGURE 34. EQUIVALENT ELECTRICAL NETWORK

constants and geometry as follows:

$$C_o = \varepsilon A/t$$

$$C_1 = 8\, C_o k^2/\pi^2 \tilde{M}^2$$

$$R_1 = \tau_1/C_1 = \pi^2 \tilde{M}^2 \eta/8\, C_o k^2 \bar{c}$$

$$L_1 = \tilde{M}^2/32\, C_o k^2 f_o^{\,2}(\tilde{M}).$$

In the above, A is the electrode area of the plate, t the plate thickness, k the piezoelectric coupling factor, $\tilde{M}$ the (odd) harmonic number, τ_1 the motional time constant, ε the dielectric permittivity, η the elastic viscosity, $\bar{c}$ the piezoelectrically stiffened elastic stiffness, and $f_o(\tilde{M})$ the nominal resonance frequency at the $\tilde{M}$th harmonic.

The effective piezoelectric constant e driving the mode in question (e_{26} for the plate thickness modes of Y-cuts) produces the stiffening of the effective elastic constant c of the mode:

$$\bar{c} = c + e^2/\varepsilon.$$

The frequency constant N for a mode is one-half the acoustic velocity of the modal waves:

$$N = (\tfrac{1}{2}) \sqrt{\bar{c}/\rho},$$

where ρ is the mass density. Because the resonance frequencies $f_o(\tilde{M})$ occur when the plate is very nearly an odd number of half-wavelengths thick,

$$f_o = (\tilde{M}/2t) \sqrt{\bar{c}/\rho} = \tilde{M}\, N/t.$$

The frequency f_o is related to the equivalent circuit parameters by

$$(2\pi\, f_o(\tilde{M}))^2 \cdot L_1\, C_1 = 1,$$

and the motional time constant is

$$\tau_1 = \eta/\bar{c} = R_1\, C_1.$$

The time constant is related to the quality factor, Q, by

$$2\pi\, f_o\, \tau_1\, Q = 1,$$

and the piezoelectric coupling factor k is obtained from

$$k^2\, \varepsilon\, \bar{c} = e^2.$$

Many of the important relationships needed to evaluate the properties

and behavior of piezoelectric vibrators are expressible in terms of normalized quantities Q, r, M and E. The capacitance ratio r for the fundamental harmonic ($\tilde{M} = 1$) is

$$r = C_o/C_1 = \pi^2/8k^2.$$

The figure of merit, M, and figure of excellence are defined as

$$M = Q/r$$

$$E = Q^2/r.$$

Electrical measurements made on the piezoelectric vibrator yield values for the equivalent circuit parameters which then permit evaluation of these auxiliary quantities.

Alpha-Aℓ PO_4 plate resonators have not yet been made to yield performance characteristics approaching those of quartz resonators[9,21]. Problems involving resonator processing are presumably a contributing factor, but material related deficiencies such as twinning and water content are probably equally important. At present, it is found that the electromechanical coupling falls between the limits

$$0.20 \leq k\ (max) \leq 0.25.$$

It therefore follows that the capacitance ratio is bounded by

$$20 < r < 30.$$

Using the presently measured range of Q values, namely,

$$10^3 < Q < 10^4,$$

we find that one of the following sets of inequalities hold:

$$E > Q > M > r, \text{ or}$$

$$E > Q > r > M.$$

The vibrator characteristics of presently available berlinite are thus such that it can be placed entirely within the classification region outlined for water-soluble piezoelectric crystals and partly within the classification region of piezoelectric refractory materials[22].

Further characterization of this material is called for in regard to a number of physical parameters, including the following: viscosities, third order elastic stiffnesses, second and third order temperature coefficients of the stiffnesses, first order temperature coefficients of the piezoelectric constants and dielectric permittivities, thermal conductivities, and specific heat. Also to be studied should be the surface properties such as etching and polishing characteristics.

The twinning properties must be regarded as potentially most important as well. With respect to resonator applications, such as filter devices, the strengths of unwanted modes, and the general complexion of the resonance mode spectrum should be investigated, along with the possible existence of a berlinite "SC-cut", where electrode stresses and thermal gradient stresses are compensated.

With the synthesis of higher purity berlinite, the above-mentioned investigations can be carried out; these will disclose the future of this promising material for frequency control and signal processing applications.

REFERENCES

1. G. A. Wolff and J. D. Broder, "Cleavage and the Identification of Minerals," Am. Mineral., Vol. 45, 1960, pp. 1230-1242.

2. R. E. Newnham, "Elastic Properties of Oxides," Ceram. Bull., Vol. 53, 1974, pp. 821-829.

3. J. D. H. Donnay and Y. LePage, "The Vicissitudes of the Low-Quartz Crystal Setting or the Pitfalls of Enantiomorphism," Acta Cryst., Vol. A34, 1978, pp. 584-594.

4. J. M. Stanley, "Hydrothermal Synthesis of Large Aluminum Phosphate Crystals," Ind. & Eng. Chem., Vol. 46, 1954, pp. 1684-1689.

5. E. D. Kolb and R. A. Laudise, "Hydrothermal Synthesis of Aluminum Orthophosphate," J. Crys. Growth, Vol. 43, 1978, pp. 313-319.

6. J. Détaint, M. Feldmann, J. Henaff, H. Poignant, and Y. Toudic, "Bulk and Surface Acoustic Wave Propagation in Berlinite," Proc. 33rd Ann. Freq. Control Symp., May-June 1979, pp. 70-79.

7. E. J. Ozimek and B. H. T. Chai, "Piezoelectric Properties of Single Crystal Berlinite," Proc. 33rd Ann. Freq. Control Symp., May-June 1979, pp. 80-87.

8. W. R. McBride and M. E. Hills, "The Hydrothermal Growth of Aluminum Orthophosphate Crystals," Fifth Intl. Conf. Cryst. Growth, Boston, MA, July 1977, Abs. 65.

9. D. F. Croxall, I. R. A. Christie, B. J. Isherwood, A. G. Todd, and J. Birch, "Growth and Assessment of Berlinite Single Crystals," Second Eur. Conf. Cryst. Growth, Lancaster, U. K., 1979.

10. T. R. AuCoin, R. O. Savage, M. J. Wade, J. G. Gualtieri, and A. Schwartz, Proc. 1980 Army Sci. Conf., June 1980, West Point, NY, Vol. I, pp. 121-133.

11. A. C. McLaren and P. P. Phakey, "A Transmission Electron Microscope Study of Amethyst and Citrine," Aust. J. Phys., Vol. 18, 1965, pp. 135-141.

12. E. Z. Arlidge, V. C. Farmer, B. D. Mitchell, and W. A. Mitchell, "Infrared, X-Ray and Thermal Analysis of Some Aluminum and Ferric Phosphates," J. Appl. Chem., Vol. 13, 1963, pp. 17-27.

13. A. Kats, "Hydrogen in Alpha-Quartz," Philips Res. Repts., Vol. 17, 1962, pp. 133-195 and 201-279.

14. L. E. Halliburton, Oklahoma State U., Stillwater, OK 74074, private communication, June 1980.

15. M. L. Shand and B. H. T. Chai, "H_2O in Berlinite Detected by Raman Scattering," J. Appl. Phys., Vol. 51, 1980, pp. 1489-1490.

16. J. C. Brice and A. M. Cole, "The Characterization of Synthetic Quartz by Using Infra-Red Absorption," Proc. 32nd Ann. Freq. Control Symp. May-June 1978, pp. 1-10.

17. A. Ballato, "Doubly Rotated Thickness Mode Plate Vibrators," in Physical Acoustics, (W. P. Mason and R. N. Thurston, eds.), Vol. 13, Chap. 5, pp. 115-181. New York: Academic, 1977.

18. IEEE Standard on Piezoelectricity: Std 176-1978, The Institute of Electrical and Electronics Engineers, Inc., 345 47th Street, New York, NY 10017.

19. Z. -P. Chang and G. R. Barsch, "Elastic Constants and Thermal Expansion of Berlinite," IEEE Trans. Sonics Ultrason., Vol. SU-23, March 1976, pp. 127-135.

20. G. K. Guttwein, T. J. Lukaszek, and A. Ballato, "Practical Consequences of Modal Parameter Control in Crystal Resonators," Technical Report ECOM-2847, US Army Electronics Command, Fort Monmouth, NJ, June 1967, 21 pp.

21. B. H. T. Chai, M. L. Shand, E. Buckler, and M. A. Gilleo, "Experimental Data on the Piezoelectric Properties of Berlinite," Proc. 1979 IEEE Ultrasonics Symp., September 1979, pp. 577-583.

22. A. Ballato, "Resonance Phenomena in Piezoelectric Vibrators," Technical Report ECOM-3181, US Army Electronics Command, Fort Monmouth, NJ, September 1969, 11 pp.

ATE
LME